Gut microbiota from patients with COVID-19 cause alterations in mice that resemble post-COVID symptoms

Viviani Mendes de Almeida
Laboratory of Microbiota and Immunomodulation - Department of Biochemistry and Immunology, Institute of Biological Sciences, Universidade Federal de Minas Gerais-UFMG, Belo Horizonte, MG, Brazil

Daiane F Engel
Department of Clinical Analysis, School of Pharmacy, Universidade Federal de Ouro Preto -UFOP, Ouro Preto, MG, Brazil

Mayra Fernanda Ricci
Laboratory of Microbiota and Immunomodulation - Department of Biochemistry and Immunology, Institute of Biological Sciences, Universidade Federal de Minas Gerais-UFMG, Belo Horizonte, MG, Brazil

Clênio Silva Cruz
Laboratory of Microbiota and Immunomodulation - Department of Biochemistry and Immunology, Institute of Biological Sciences, Universidade Federal de Minas Gerais-UFMG, Belo Horizonte, MG, Brazil

Icaro Santos Lopes
Laboratory of Virus Bioinformatics - Department of Biological Science, Center of Biotechnology and Genetics, Universidade Estadual de Santa Cruz-UESC, Ilhéus, BA, Brazil.

Daniele Almeida Alves
Laboratory of RNA interference and antiviral immunity - Department of Biochemistry and Immunology, Institute of Biological Sciences, Universidade Federal de Minas Gerais-UFMG, Belo Horizonte, MG, Braz

Mirna d' Auriol
Laboratory of Toxicology - Departament of Clinical and Toxicological Analysis, Faculty of Pharmacy, Universidade Federal de Minas Gerais-UFMG, Belo Horizonte, MG, Brazil

João Magalhães
Laboratory of Microbiota and Immunomodulation - Department of Biochemistry and Immunology, Institute of Biological Sciences, Universidade Federal de Minas Gerais-UFMG, Belo Horizonte, MG, Brazil

Giuliana S. Zuccoli
Laboratory of Neuroproteomics - Department of Biochemistry and Tissue Biology, Institute of Biology, State University of Campinas- UNICAMP, Campinas, SP, Brazil.

Bradley Joseph Smith
Laboratory of Neuroproteomics - Department of Biochemistry and Tissue Biology, Institute of Biology, State University of Campinas- UNICAMP, Campinas, SP, Brazil.

Victor Corasolla Carregari

Laboratory of Neuroproteomics - Department of Biochemistry and Tissue Biology, Institute of Biology, State University of Campinas- UNICAMP, Campinas, SP, Brazil.

Elayne Cristina Machado

Laboratory of Microbiota and Immunomodulation - Department of Biochemistry and Immunology, Institute of Biological Sciences, Universidade Federal de Minas Gerais-UFMG, Belo Horizonte, MG, Brazil

Victor M. Rocha

Laboratory of Microbiota and Immunomodulation - Department of Biochemistry and Immunology, Institute of Biological Sciences, Universidade Federal de Minas Gerais-UFMG, Belo Horizonte, MG, Brazil

Toniana G. Carvalho

Laboratory of Neurobiochemistry - Department of Biochemistry and Immunology, Institute of Biological Sciences, Federal University of Minas Gerais, Belo Horizonte, MG, Brazil.

Larisse de Souza Barbosa Lacerda

Center for Research and Development of Drugs - Department of Morphology, Institute of Biological Sciences, Universidade Federal de Minas Gerais-UFMG, Belo Horizonte, MG, Brazil

Jordane C. Pimenta

Center for Research and Development of Drugs - Department of Morphology, Institute of Biological Sciences, Universidade Federal de Minas Gerais-UFMG, Belo Horizonte, MG, Brazil

Izabela Galvão

Laboratory of Microbiota and Immunomodulation - Department of Biochemistry and Immunology, Institute of Biological Sciences, Universidade Federal de Minas Gerais-UFMG, Belo Horizonte, MG, Brazil

Mariana Aganetti Silva

Laboratory of Microbiota and Immunomodulation - Department of Biochemistry and Immunology, Institute of Biological Sciences, Universidade Federal de Minas Gerais-UFMG, Belo Horizonte, MG, Brazil

Erika da Silva Rosa

Laboratory of Microbiota and Immunomodulation - Department of Biochemistry and Immunology, Institute of Biological Sciences, Universidade Federal de Minas Gerais-UFMG, Belo Horizonte, MG, Brazil

Geovanni Dantas Cassali

Laboratory of Comparative Pathology - Department of Pathology, Universidade Federal de Minas Gerais-UFMG, Belo Horizonte, MG, Brazil.

Cristiana C. Garcia

Laboratory of Respiratory Viruses and Measles, Instituto Oswaldo Cruz, Fiocruz, Rio de Janeiro, RJ, Brazil

Mauro Martins Teixeira

Center for Research and Development of Drugs - Department of Morphology, Institute of Biological Sciences, Universidade Federal de Minas Gerais-UFMG, Belo Horizonte, MG, Brazil

Leiliane Coelho

Laboratory of Toxicology - Departament of Clinical and Toxicological Analysis, Faculty of Pharmacy, Universidade Federal de Minas Gerais-UFMG, Belo Horizonte, MG, Brazil

Fabiola Mara Ribeiro

Laboratory of Neurobiochemistry - Department of Biochemistry and Immunology, Institute of Biological Sciences, Federal University of Minas Gerais, Belo Horizonte, MG, Brazil.

Flaviano S. Martins

Laboratory of Biotherapeutic Agents - Department of Microbiology, Institute of Biological Sciences, Universidade Federal de Minas Gerais-UFMG, Belo Horizonte, MG, Brazil

Rafael Simone Saia

Laboratory of Intestinal Physiology - Department of Physiology, Ribeirão Preto Medical School, Universidade de São Paulo, Ribeirão Preto, SP, Brazil.

Vivian Vasconcelos Costa

Center for Research and Development of Drugs - Department of Morphology, Institute of Biological Sciences, Universidade Federal de Minas Gerais-UFMG, Belo Horizonte, MG, Brazil

Daniel Martins-de-Souza

Laboratory of Neuroproteomics - Department of Biochemistry and Tissue Biology, Institute of Biology, State University of Campinas- UNICAMP, Campinas, SP, Brazil.

João T. Marques

Laboratory of RNA interference and antiviral immunity - Department of Biochemistry and Immunology, Institute of Biological Sciences, Universidade Federal de Minas Gerais-UFMG, Belo Horizonte, MG, Braz

Eric R. G. R. Aguiar

Laboratory of Virus Bioinformatics - Department of Biological Science, Center of Biotechnology and Genetics, Universidade Estadual de Santa Cruz-UESC, Ilhéus, BA, Brazil.

Angelica T. Vieira (angelicathomazvieira@ufmg.br)

Laboratory of Microbiota and Immunomodulation - Department of Biochemistry and Immunology, Institute of Biological Sciences, Universidade Federal de Minas Gerais-UFMG, Belo Horizonte, MG, Brazil

---

Research Article

Keywords: COVID-19, SARS-CoV-2, Post-COVID, Microbiota, Inflammation, Antimicrobial-resistance

Posted Date: April 12th, 2023

DOI: https://doi.org/10.21203/rs.3.rs-1756189/v2

Additional Declarations: No competing interests reported.

Article

Gut microbiota from patients with COVID-19 cause alterations in mice that resemble post-COVID symptoms

Viviani Mendes de Almeida[1*], Daiane F. Engel[2*], Mayra F. Ricci[1*], Clênio Silva Cruz[1], Ícaro Santos Lopes[3], Daniele Almeida Alves[4], Mirna d' Auriol[5], João Magalhães[1], Elayne C. Machado[1], Victor M. Rocha[1], Toniana G. Carvalho[7], Larisse de S. B. Lacerda[8], Jordane C. Pimenta[8], Mariana Aganetti[1], Giuliana S. Zuccoli[6], Bradley J. Smith[6], Victor C. Carregari[6], Erika da Silva Rosa[1], Izabela Galvão[1], Geovanni Dantas Cassali[9], Cristiana C. Garcia[10], Mauro Martins Teixeira[8], Leiliane C. André[5], Fabiola Mara Ribeiro[7], Flaviano S. Martins[11], Rafael Simone Saia[12], Vivian Vasconcelos Costa[8], Daniel Martins-de-Souza[6,13,14,15], Philip M. Hansbro[16], João Trindade Marques[4,17], Eric R. G. R. Aguiar[3], Angélica T. Vieira[1#]

[1]Laboratory of Microbiota and Immunomodulation - Department of Biochemistry and Immunology, Institute of Biological Sciences, Universidade Federal de Minas Gerais - UFMG, Belo Horizonte, MG, Brazil.

[2]Department of Clinical Analysis, School of Pharmacy, Universidade Federal de Ouro Preto - UFOP, Ouro Preto, MG, Brazil.

[3]Laboratory of Virus Bioinformatics - Department of Biological Science, Center of Biotechnology and Genetics, Universidade Estadual de Santa Cruz - UESC, Ilhéus, BA, Brazil.

[4]Laboratory of RNA Interference and Antiviral Immunity - Department of Biochemistry and Immunology, Institute of Biological Sciences, Universidade Federal de Minas Gerais - UFMG, Belo Horizonte, MG, Brazil.

[5]Laboratory of Toxicology - Department of Clinical and Toxicological Analysis, Faculty of Pharmacy, Universidade Federal de Minas Gerais - UFMG, Belo Horizonte, MG, Brazil.

[6]Laboratory of Neuroproteomics - Department of Biochemistry and Tissue Biology, Institute of Biology, Universidade do Estado de Campinas - UNICAMP, Campinas, SP, Brazil.

[7]Laboratory of Neurobiochemistry - Department of Biochemistry and Immunology, Institute of Biological Sciences, Universidade Federal de Minas Gerais - UFMG, Belo Horizonte, MG, Brazil.

[8]Center for Research and Development of Drugs - Department of Morphology, Institute of Biological Sciences, Universidade Federal de Minas Gerais - UFMG, Belo Horizonte, MG, Brazil

[9]Laboratory of Comparative Pathology - Department of Pathology, Universidade Federal de Minas Gerais - UFMG, Belo Horizonte, MG, Brazil.

[10]Laboratory of Respiratory Viruses and Measles, Instituto Oswaldo Cruz - Fiocruz, Rio de Janeiro, RJ, Brazil

[11]Laboratory of Biotherapeutic Agents - Department of Microbiology, Institute of Biological Sciences, Universidade Federal de Minas Gerais - UFMG, Belo Horizonte, MG, Brazil

[12]Laboratory of Intestinal Physiology - Department of Physiology, Ribeirão Preto Medical School, Universidade de São Paulo, Ribeirão Preto, SP, Brazil.

[13]D'Or Institute for Research and Education, São Paulo, SP, Brazil;

[14]Experimental Medicine Research Cluster – Universidade do Estado de Campinas - UNICAMP, Campinas, SP, Brazil;

[15]National Institute of Biomarkers in Neuropsychiatry - National Council for Scientific and Technological Development, São Paulo, SP, Brazil;

[16] Centre for Inflammation, Centenary Institute and University of Technology Sydney, School of Life Sciences, Faculty of Science, Sydney, NSW, Australia

[17]University of Strasbourg, CNRS UPR9022, INSERM U1257, Strasbourg 67084, France.

***These authors contributed equally to this work**

#Correspondence:

ORCID: https://orcid.org/0000-0002-4556-7671

Professor Angelica Thomaz Vieira, Laboratory of Microbiota and Immunomodulation - Institute of Biological Sciences, Universidade Federal de Minas Gerais - UFMG, Av. Pres. Antônio Carlos, 6627 - Pampulha, Belo Horizonte, MG, Brazil - ZipCode: 31270-901

phone: +55 31 3409-3047 angelicathomazvieira@ufmg.br

Abstract

Long-term sequelae after Coronavirus disease (COVID)-19 are frequent and of major concern. SARS-CoV-2 infection affects the host's gut microbiota, which is linked with disease severity in patients with COVID-19. We report here that the gut microbiota of post-COVID subjects had a remarkable predominance of *Enterobacteriaceae* strains with antibiotic-resistance phenotype compared to healthy controls. Additionally, short-chain fatty acids (SCFA) levels were reduced in their feces. Fecal transplant from post-COVID subjects to germ-free mice led to lung inflammation and worst outcomes during pulmonary infection by multidrug-resistant *Klebsiella pneumoniae.* Transplanted mice also had poorer cognitive performance. Overall, we show prolonged impacts of SARS-CoV-2 infection in the gut microbiota that persist after subjects have cleared the virus. Together, these data demonstrate that the gut microbiota can directly contribute to post-COVID sequelae, suggesting that it may be a potential therapeutic target.

Keywords: COVID-19, SARS-CoV-2, Post-COVID, Microbiota, Inflammation, Antimicrobial-resistance.

Introduction

The newly emerged β-coronavirus, severe acute respiratory syndrome-coronavirus-2 (SARS-CoV-2) has caused more than 618 million confirmed cases and 6,8 million deaths globally as of March 2023 (WHO, 2023). After clearance of SARS-CoV-2, long-term complications of coronavirus disease-2019 (COVID-19) are common even among patients that had mild or asymptomatic disease during the acute phase (Augustin et al., 2021; Johansen et al., 2022; Lopez-Leon et al., 2021; Subramanian et al., 2022). SARS-CoV-2 requires the angiotensin-converting enzyme 2 (ACE2) and Transmembrane Serine Protease 2 (TMPRSS2) to infect lung cells (Hikmet et al., 2020). The gastrointestinal tract expresses high levels of these receptors and is also vulnerable (Sencio et al., 2021; Yeoh et al., 2021). The gut microbiota has been shown to influence COVID-19 severity and post-COVID long-term effects (Yeoh et al., 2021; Zuo et al., 2021).

The human gut microbiome includes trillions of microorganisms, primarily bacteria, forming a complex and well-recognized ecosystem. An imbalance in gut microbiota composition referred to as dysbiosis, is a major factor in disease development and can be caused by viral infections and other respiratory challenges (Chen et al., 2022; Cullen, 2013; Wu et al., 2021a; Zuo et al., 2021). Individuals who experience severe COVID-19 have reduced diversity and abundance of commensal gut microbiota (Chen et al., 2022; Liu et al., 2022; Zollner et al., 2022). Dysbiosis of the gut microbiota was observed up to 1 year after the initial infection and virus clearance post-COVID (Liu et al., 2022). Thus, these long-term changes in gut microbiota could contribute to the symptoms of long-COVID, but there is currently no direct evidence for this link (Bowermicrobiomeman et al., 2020; Fernández-de-Las-Peñas et al., 2021).

Here, we investigated whether the gut microbiota derived from individuals previously infected with SARS-CoV-2 who had mild or no symptoms could induce post-COVID consequences. To investigate this, we performed human fecal microbiota transference to germ-free mice as an experimental approach. Our data provide evidence that gut microbiota from COVID-19 patients can cause sequelae from infection in the absence of SARS-CoV-2, including induction of lung inflammation and brain dysfunction.

Results

Comparison of clinical, dietary, and microbiological parameters between controls (non-COVID) and post-COVID subjects

We recruited a total of 131 volunteers: seventy-two (55%) subjects had SARS-CoV-2 infection (post-COVID group), and fifty-nine (45%) subjects were COVID-19-naïve healthy control subjects (Figure 1A). The experimental design and clinical characteristics of all subjects are summarized in Figure 1—figure supplement 1 and Table 1, respectively. Among the post-COVID subjects: sixty-four (89%) had mild/moderate illness during the symptomatic period, and feces were collected between 1 to 4 months after initial symptoms. Additionally, thirty-one (48%) post-COVID subjects reported experiencing gastrointestinal symptoms during SARS-CoV-2 infection (Table 1). Eight volunteers (11%) had confirmed exposure to SARS-CoV-2 by serological methods (at the time the samples were collected when vaccines were unavailable) but were asymptomatic. Factors affecting gut microbiota between the two groups, including pre-existing comorbidities, such as hypertension, hypothyroidism, irritable bowel disease, and chronic respiratory diseases were similar between post-COVID individuals and controls (Figure 1B). Dietary habits were also similar between the groups (Figure 1C). The use of antibiotics (three months before and during SARS-CoV-2 infection) was reported in 24 (33%) of post-COVID subjects and 7 (12%) of control subjects, with significant differences between both groups (Figure 1D). Of note, all fecal samples tested negative for SARS-CoV-2 nucleic acid by RT-qPCR at the time of collection (Figure 1E).

Gut microbiota composition was analyzed by 16S sequencing in 44 fecal samples prioritizing sampling of paired subjects from the same household (15 families) see samples workflow in (Figure 1—figure supplement 1B). We attempted to sample paired subjects from the same family since human-associated microbiota communities vary across individuals, but cohabiting family members share a similar microbiota with each other (Caugant et al., 1984; Song et al., 2013). Analysis of the gut microbiota revealed similar profiles between individual samples from controls and post-COVID subjects (Figure 1F). β-diversity (weighted UniFrac distances) and α-diversity metrics (Shannon, Simpson, and Chao1 indexes) showed no significant differences in the gut microbiota between groups, indicating similar taxonomic diversity (Figure 1F).

To explore the possible impact of SARS-CoV-2 infection on the gut microbiota beyond its composition, we evaluated the frequency of cultivable *Enterobacteriaceae* – due to their importance as pathobionts that serve as a reservoir of antimicrobial resistance genes of clinical interest – comparing the total amount of colony forming unit (CFU) in the feces between controls x post-COVID subjects. Despite similar CFU numbers between the two groups (Figure 1G), post-COVID subjects had a higher percentage of *Enterobacteriaceae* strains with a drug-resistant (45% DR) and multidrug-resistant (23% MDR) phenotype when compared to controls (39% DR and 13% MDR) (Figure 1H). We identified an increased prevalence of *Klebsiella* sp among all Enterobacteriaceae strains assessed. AMR over *Escherichia* sp. in post-COVID subjects compared to controls (Figure 1—figure supplement 1C). These *Klebsiella* strains were predominantly resistant to quinolones (64%), aminoglycosides (100%), and sulfonamides (91%) (data not shown), which are not associated with intrinsic resistance in this bacterial genus. Overall, these findings show increased AMR in the *Enterobacteriaceae* community of the gut microbiota post-COVID, which might be partly due to the increased overuse of antibiotics treatment in this subject group but could also be a direct effect of the SARS-CoV-2 infection, although the mechanisms remain unclear.

Post-COVID microbiota-induced alterations in the gut of microbiota humanized mice

To understand the direct contribution of post-COVID microbiota to the host, we performed human fecal microbiota transplant (FMT) to germ-free mice. Fecal samples were harvested from controls and post-COVID volunteers (Figure 2A), prioritizing samples belonging to the same family (co-housing human fecal samples) (Figure 1—figure supplement 1B) to minimize differences in the gut microbiota caused by other environmental factors. The FMT was performed from each human microbiota donor transfer to individual germ-free mice (Figure 2—figure supplement 1A). After FMT, mice were housed for 10 to 12 days to stabilize the human-derived microbiota. This protocol utilized was based on previous work from our group, where we observed reversal hyporesponsiveness to inflammatory stimulus in germ-free mice after 7 days of fecal transplantation (M C C et al., 2014; Pedroso et al., 2015; Rungue et al., 2021; Souza et al., 2004). Nevertheless, there is no scientific

consensus on the best methodology and timing of colonization for FMT to germ free mice.

We evaluated the human donor microbiota engraftment, first by comparing the differences in β and α-diversity observed between fecal samples from human donors versus recipient mice (Figure 2B). Besides the differences between microbiota from human donors and recipient germ-free mice, transplanted humanized mice showed similarities between controls and post-COVID groups for both β and α-diversity (Figure 2C). When comparing the composition and abundance of individual bacterial groups in the gut microbiota of transplanted humanized mice, the *Lachnospiraceae* family significantly increased in post-COVID compared to the control (Figure 2D). Although *Lachnospiraceae* were present in both inoculum of feces from donors, there were no differences between control and post-COVID subjects (data not shown).

FMT can be used to demonstrate a direct effect of the gut microbiota in physiological process. We, therefore, analyzed the impact of human microbiota in the gut of humanized microbiota (HM) mice comparing those that received feces from post-COVID *versus* control subject donors. HM mice that received feces from post-COVID subject donors did not show structural changes in the small intestine compared to controls but exhibited augmented cecal patches and an increase of goblet cells in the colon (Figure 2E).

To gain insights into the role of gut microbiota from post-COVID donors that may compromise intestinal homeostasis and may influence systemic inflammation, we collected blood from the human donors. We observed higher levels of I-FABP, a marker of epithelial damage (Figure 2—figure supplement 1B), suggesting disturbs on the gut epithelial barrier integrity in post-COVID subjects. However, this did not lead to increased translocation of gram-negative bacteria from the gut since we did not observe differences in LPS levels in the serum between groups (Figure 2—figure supplement 1C). Consistent with previous findings (Zhang et al., 2022), the levels of commensal microbial metabolites (acetate, propionate, butyrate) were reduced in fecal samples of post-COVID subjects compared to their paired controls (Figure 2—figure supplement D-F). These findings suggest that post-COVID subjects had signs of intestinal epithelial injury with increased circulating I-FABP levels that might influence extra-intestinal organs.

Post-COVID gut microbiota induces histological changes in the lung of humanized microbiota mice

To explore the systemic impact of post-COVID gut microbiota to extra-intestinal organs, we next assessed the effects of FMT on the lung of recipient HM mice 12 days after the transplant (Figure 3A). We found foci of inflammatory infiltrate, mostly neutrophils, in both perivascular/peri-bronchial regions and increased histopathology score in the lung of mice receiving feces from post-COVID patients (Figure 3B). In addition, post-COVID mice increased the expression of α-smooth muscle actin (α-SMA), indicative of lung physiological dysfunction (Figure 3B). Also, they had increased inflammatory cells in the broncheoalveolar fluid (BAL) compared to controls (Figure 3C). Cultivable *Enterobacteriaceae* in the BAL from post-COVID mice were found in higher levels than control animals (Figure 3D), suggesting increased translocation of bacteria from the gut to the lung that may account for the observed phenotype. Of note, there was no detection of SARS-CoV-2 nucleic acid in lung tissues (Figure 3E), which corroborates the absence of the virus in fecal samples used for the initial transplant (Figure 1E).

Overall, our data indicate that transference of fecal samples from post-COVID subjects induced lung inflammation in recipient mice in the absence of SARS-CoV-2, suggesting that the intestinal microbiota modified by COVID-19 causes this phenotype.

Fecal transplantation from post-COVID human volunteers to HM mice impairs host pulmonary defense

We hypothesized that the consequences of post-COVID fecal transplant-induced lung alterations can further impact host defense and favor secondary infections. To validate this hypothesis, we performed intranasal infections of HM mice with a multidrug-resistant strain of *Klebsiella pneumonia (Kp)* (Figure 4A). We compared *Kp* lung infection in control *versus* post-COVID mice and observed higher pathological changes in the perivascular, peri-bronchial, and parenchyma characterized by emphysema-like areas in the lung of infected post-COVID mice (Figure 4B). These changes were associated with an intense inflammatory cell infiltration in the BAL of those mice when compared to infected control mice (Figure 4C). Despite it, the recruitment of inflammatory cells to the lung was inefficient for the clearance of the bacteria since we harvested similar CFU levels of *Kp* in the lung of

both control and post-COVID-infected mice (Figure 4D). Our group and others demonstrated that acetate, a gut microbiota metabolite, contributes to controlling pulmonary infection induced by the pathogen *Klebsiella pneumonia* in mice (Galvão et al., 2018; Vieira et al., 2016b; Wu et al., 2020). Accordingly, we observed reduced serum acetate levels in post-COVID *Kp*-infected mice compared to post-COVID non-infected (vehicle) mice (Figure 4E). Overall, our data indicate that transplant of post-COVID feces affected the lungs of recipient mice in the absence of SARS-CoV-2 and contributed to the impairment of the host's lung defense against bacterial infection.

Post-COVID gut microbiota induces memory impairment and hippocampus changes and can be partially reversed with probiotic

Beyond the lung alterations, accumulating reports have found that post-COVID sequelae are commonly associated with brain dysfunction (Douaud et al., 2022; Hartung et al., 2022; Heine et al., 2023; Liu et al., 2022). To further explore the causal effects of gut microbiota on brain alterations, HM germ-free mice that received FMT from post-COVID and control subjects were subjected to cognitive behavioral tests (Figure 5A). Post-COVID mice showed memory impairment in recognition and location tests compared to controls mice (Figure 5B). Control mice showed significantly more interaction with a novel object in the cage when compared to post-COVID mice. Based on these phenotypes, we analyzed inflammatory markers in the hippocampus of post-COVID mice that could indicate a possible connection with neuroinflammation. We observed increased mRNA expression of the pro-inflammatory cytokine *tnf* but lower levels of neuroprotective factors such as, *bdnf* and *psd-95* in post-COVID mice when compared to controls (Figure 5C-E). Together these results suggest that the alterations in the gut microbiota and inflammation caused by COVID-19 can directly cause changes in brain cognition.

To further investigate and test the potential of microbiota-based interventions as a target to prevent the memory impairment induced by direct coronavirus infection, we used a β-coronavirus murine model of lung infection (Andrade et al., 2021). This experimental murine model with mouse hepatitis virus (MHV-3) mimics human COVID-19 inflammatory manifestations in mice and we also observed that infected animals had memory impairment using the object location test. Using this model, we tested the potential of microbiome-based interventions by administering

the probiotic *Bifidobacterium longum* 5^{1A} (Figure 6A). Treatment with *B. longum* 5^{1A} prevented memory impairment induced by MHV-3 infection in mice (Figure 6B).

Altogether, our data indicate that alterations in the gut microbiota contribute to post-COVID disruption of hippocampal function leading to cognitive impairment, which might be prevented or attenuated via microbiome-based interventions.

Discussion

Among pathophysiological responses triggered by SARS-CoV-2 infection, several studies showed associations between gastrointestinal symptoms and altered gut microbiota in COVID-19 during and after the infection (Liu et al., 2022; Livanos et al., 2021; Merad et al., 2022; Wu et al., 2021b; Xu et al., 2023). However, our study is the first to show a causal effect of gut microbiota alterations in post-COVID sequalae. Our findings confirm previous data that SARS-CoV-2 infection is associated with spread of antimicrobial resistance in gut microbiota (Bernard-Raichon et al., 2022; de Nies et al., 2023; Kariyawasam et al., 2022; Langford et al., 2022a, 2022b; López-Jácome et al., 2022). In fact, we observed the increase of AMR *Enterobacteriaceae* in the gut microbiota of post-COVID individuals who were either asymptomatic or had mild symptoms of COVID-19. This is especially surprising as the COVID-19-related AMR spread has been mainly associated with moderate/severe cases and hospitalized individuals (Kariyawasam et al., 2022). Although the widespread use of antimicrobials during COVID-19 and overuse between our post-COVID and control volunteers may explain the increased AMR spread (Furlan and Caramelli, 2021; Jeon et al., 2022; Karami et al., 2021; Van Laethem et al., 2022), we do not exclude the direct impact of SARS-CoV-2 infection on increasing AMR through the microbiome. Of note, we found a predominant increase of AMR *Klebsiella* sp. in post-COVID gut microbiota subjects. This bacterium belongs to the ESKAPE group: *Enterococcus faecium, Staphylococcus aureus, Klebsiella pneumoniae, Acinetobacter baumannii, Pseudomonas aeruginosa, and Enterobacter species*) of AMR pathogenic bacteria that is responsible for most nosocomial pneumonia in hospitalized patients with COVID-19 (Bazaid et al., 2022; Russell et al., 2021). Moreover, post-COVID mice had worse lung injury, which compromised the lung immune response to *K. pneumoniae* B31 infection. Therefore, the post-COVID microbiota transference may have contributed to the impairment of the pulmonary immune system inducing a greater susceptibility

to infections caused by pathogens/pathobionts (Arcari et al., 2021; Chong et al., 2021; Gerver et al., 2021; Protonotariou et al., 2022). Another relevant factor related to pulmonary alterations observed in post-COVID mice is lung microbiota disruption (Zheng et al., 2020). Lung microbiota is known to be susceptible to gut microbiota alterations, highlighting the relevance of the gut-lung axis (Jang et al., 2021; Zheng et al., 2020). Although we did not evaluate the lung microbiota as a whole, we found increased cultivable *Enterobacteriaceae* in the lungs and pulmonary tissue damage in mice with post-COVID gut microbiota but not in controls. These findings raise questions about the components in the fecal samples that induced such alterations after transplantation and which mechanisms are involved in the gut-lung connection.

The next step in our investigation was to deepen our understanding of the effects triggered by the post-COVID microbiota by exploring other host tissues. Therefore, the connection between the gut and brain is well established (Sampson and Mazmanian, 2015), and most recently, it has been described as the lung-brain axis (Bajinka et al., 2022; Hosang et al., 2022). Our findings that post-COVID microbiota can induce memory impairment in transplanted mice suggested a possible connection with the neurological outcomes of post-acute COVID in humans (Monje and Iwasaki, 2022; Taquet et al., 2021). Although our study did not assess the role of lung microbiota in neurological disorders, clinical studies show differences in the lung microbiota in cognitively impaired individuals *versus* controls (Yang et al., 2021). Previous studies suggested that even minimal alterations in the lung microbiome can affect the central nervous system, although significant changes in gut microbiota were necessary (Erny et al., 2015). Thus, lung alterations induced by microbiota of post-COVID human donors in post-COVID mice may be associated with neurological outcomes.

Gut microbiome production of metabolites, particularly SCFA, is an effective mechanism that support the gut-lung and gut-brain axis (Bowermicrobiomeman et al., 2020; Dang and Marsland, 2019). SCFAs are also known to act in the development of the immune system and lung mucosal function, protecting against infections and pulmonary damage (Dang and Marsland, 2019). Furthermore, SCFA can also modulate blood-brain barrier integrity and inflammatory responses in microglia (Erny et al., 2015), and clinical and experimental studies associated reduced SCFA levels with Alzheimer's disease (Doifode et al., 2021). We found reduced acetate, propionate, and butyrate levels in the feces of post-COVID donor

subjects and decreased acetate in post-COVID *Kp*-infected mice. Thus, this decrease in SCFA levels could affect the gut-lung and gut-brain connections and help explain neurological sequelae and the increased susceptibility to pulmonary coinfections observed in post-COVID.

We also observed apparent differences in the systemic levels of host factors, such as I-FABP, indicating loss of intestinal homeostasis in post-COVID subjects compared to controls. Indeed, I-FABP is a relevant prognostic biomarker that is positively correlated with a worse prognosis for COVID-19 (Saia et al., 2021). Thus, although no significant differences in α and β-diversity were observed in the gut microbiota of post-COVID and control subjects, functional changes were observed in both patients and mice. Of note, enrichment of the *Lachnospiraceae* family in post-COVID mice is corroborated by previous findings where subjects with COVID-19 had a higher prevalence of this group of bacteria (Al Bataineh et al., 2021; Mańkowska-Wierzbicka et al., 2023).

We observed increased TNF expression in the hippocampus of mice with post-COVID gut microbiota, suggesting neuroinflammatory responses in the central nervous system. A similar effect occurred in a colitis model, where systemic-driven TNF hippocampal expression was associated with memory impairment, which was abolished upon restoring the gut microbiota (Jang et al., 2018). Furthermore, we found reduced expression of the neuroplasticity markers BDNF and PSD-95 in the hippocampus of post-COVID mice. This impairment in neuroplasticity was previously observed when feces from transgenic Alzheimer's disease mice transferred the cognitive phenotype to recipient mice (Kim et al., 2021).

As a proof-of-concept for the potential use of microbiome-based approaches for post-COVID sequelae, we used a probiotic strain of *B. longum* 5^{1A} to assess a mouse model of coronavirus infection. Here we used the probiotic *B. longum* 5^{1A}, isolated from the gut microbiota of healthy children, which can produce high levels of SCFAs, and has beneficial effects in controlling inflammation at a systemic level, especially in the lung (da Silva et al., 2021; A.T. Vieira et al., 2015; Vieira et al., 2016a). We observed the neuroprotective effects of *B. longum* 5^{1A} that prevented memory impairment after lung infection by a murine coronavirus. Although the effects of *B. longum* 5^{1A} should be explored further, these data suggest that therapies targeting the gut microbiota are promising approaches to treat post-acute COVID-19 consequences (Alharbi et al., 2022).

Our study indicates a direct connection between altered gut microbiota and post-COVID symptoms (Fernández-de-Las-Peñas et al., 2021). Nevertheless, there are some limitations that should be taken into account. First, our study had a relatively small sample size and compared humans that were not perfectly age- and sex-matched. Other factors, such as gut viromes, were not assessed in our study but have been associated with clinical outcomes of COVID-19 (Lu et al., 2021; Mukhopadhya et al., 2019; Yuan et al., 2020; Zuo et al., 2021). Finally, SARS-CoV-2 antigens can persist for long periods in the intestine, feces, and gut tissues, boosting immune responses that may fuel post-COVID symptoms (Natarajan et al., 2022). However, we did not detect SARS-CoV-2 in the feces of donors or the lungs of humanized microbiota mice.

Collectively, our results suggest a direct connection between the long-term effects of COVID-19 with alterations in gut microbiota after clearance of SARS-CoV-2 infection. Our findings emphasize the need to define how the gut microbiota is affected by SARS-CoV-2 infection even in those that do not have severe symptoms. This is especially important given the increased AMR in the gut microbiota of those previously infected with SARS-CoV-2. AMR has been spreading at alarming rates and the effects of the COVID-19 pandemic on the gut microbiota resistome could have a major additional contribution.

Materials and methods

Study design

This cross-sectional study consisted of two steps: **1.** fresh feces and blood were collected from post-COVID and health volunteers (Control), and a survey consisting of clinical symptoms during COVID-19, medication use, and lifestyle questions was applied (Figure 1—figure supplement 1A); **2.** We developed humanized-microbiota (HM) mice by performing individual FMT from these donors into GF recipient mice (Figure 2—figure supplement 1F). For the FMT, samples of subjects (Control and Post-COVID) from the same household (n=6 families; in total n=12 members) were prioritized, where one was post-COVID and the other was not infected (Control). Additionally, random samples of post-COVID individuals (n=8) were added to the experimental n, totaling n=19 samples. In addition to the second stage of the study, an experimental pulmonary infection induced by the multidrug-resistant *Klebsiella pneumoniae* B31 strain was also performed (Figure 4A).

Study subjects and sample collection

Seventy-two post-COVID volunteers (after nucleic acid amplification test [NAAT] or an antigen test confirmed SARS-CoV-2 infection) and fifty-nine control volunteers (SARS-CoV-2 NAAT or antigen and IgG/IgM negative) were included (Figure 1—figure supplement 1A). Among the post-COVID group, sixty-four volunteers were symptomatic (collections were performed 1 to 4 months after infection), and eight were asymptomatic (classified after antigen test). All volunteers, control and post-COVID were between 15 and 60 years old. The clinical spectrum of disease severity (mild and moderate) in post-COVID and the volunteers were classified according to the NIH COVID-19 Treatment Guidelines (National Institutes of Health, 2022). Vaccination for SARS-CoV-2 and a positive serological test at the time of sample collection were the exclusion criteria. Samples were collected between October 2020 - April 2021 in Belo Horizonte - Minas Gerais, Brazil. Fecal samples were self-collected in a sterile container and immediately stored in a home refrigerator (4^{o}C) for 12 hours maximum prior to analyzes and FMT in the laboratory. All subjects consented to participate in this study under approval from the Ethics Committee on Human Research of Universidade Federal de Minas Gerais (COEP) protocol 4.615.698.

SARS-CoV-2 load in fecal samples

RNA extraction from feces, human and mouse samples, was adapted from a previously published protocol (Coryell et al., 2021). Briefly, fecal samples were diluted 1:5 (w:v) in guanidine, homogenized, and clarified by centrifugation (4,000x*g*, 20 min, 4°C). Viral RNA was purified using QIAamp Viral RNA Mini Kits following the manufacturer's instructions. RT-qPCR for SARS-CoV-2 used the one-step RT-qPCR Master Mix according to the CDC USA protocol (CDC, 2020) and primers for N1 and N2 (cat. no. 10006770) in in the QuantStudio™ 7 Flex real-time PCR system platform (Applied Biosystems, USA). For analysis, amplification values of N1 or N2 viral targets with threshold cycle (Ct) below 40.0 were considered positive for SARS-CoV-2, and above 40 or indeterminate were considered as undetectable, and the relative concentrations were expressed in arbitrary units. Fecal samples spiked with inactivated SARS-CoV-2 (stock titer 6.7x10^{6} PFU/mL) were used as a positive control at different dilutions.

Gut microbiota composition analysis

DNA extractions of fecal samples – human and mouse – stored at -70°C were performed using QIAamp DNA Stool Mini Kits (Qiagen, USA) according to the manufacturer's instructions. DNA was used as a template in PCR amplicon targeting the V3 and V4 hypervariable regions of the bacterial 16S rRNA gene. The Illumina 16S Metagenomic Sequencing Library Preparation protocol was used to prepare the 16S rRNA gene library. The 16S library was quantified by Qubit dsDNA HS Assay Kit (Invitrogen, USA) and checked with a 2100 Bioanalyzer Instrument (Agilent Technologies, USA). The sample pool (4 nM) library was diluted further final concentration of 8 pM and added to 20% (v/v) of 8 pM PhiX DNA (Illumina, USA), following Illumina guidelines. Sequencing was performed using the Miseq reagent kit v3 (600 cycles) in the Illumina MiSeq platform and 2×300 bp (MSC v2.4) according to the manufacturer's instructions (Illumina, USA). The 16S rRNA gene sequence data was processed using the QIIME2 pipeline (Bolyen et al., 2019). First, sequenced reads were denoised with DADA2 and then processed by VSEARCH (Rognes et al., 2016) to filter eventual chimeras and perform de novo clustering of valid sequences into OTUs requiring 97% sequence similarity. Next, MAFFT Fasttree was applied to conduct phylogenetic analysis based on OTUs. α and β – diversity were analyzed using the core-metrics-phylogenetic method built-in to QIIME2: for α-diversity, Shannon and Simpson diversity indices and Chao1 were calculated; for β-diversity, Bray-Curtis and weighted UniFrac distances were calculated. OTUs were taxonomically classified using Naive Bayes classifiers trained with Silva v. 138, setting 97% of sequence similarity for full-length OTUs. Differential abundance was calculated using ANCOM (Quast et al., 2012). Two-sided alternative Wilcoxon test was performed for alpha-diversity parameters, while pairwise Permanova was performed for beta-diversity parameters. Differential bacterial abundance was calculated using DESeq2 (Love et al., 2014) and plotted as a Volcano plot using EnhancedVolcano package (Blighe, Kevin, Sharmila Rana, 2019). Bacterial family with log2 Fold-change > 0,5 and P-value ≤ 0.05 was considered statistically different between conditions. Statistical analyzes were performed using in the R statistical software environment (The R Foundation, Austria). The 16S rRNA gene amplicon sequencing library produced in this work was deposited in the NCBI SRA database under project number PRJNA843134.

Enterobacteriaceae identification and Antimicrobial Resistance Test

Fresh feces samples were homogenized (100 mg for each 1 mL of sterile 0.9% saline) and serially diluted (1:10). Subsequently, different dilutions were plated on MacConkey agar (Sigma, Germany) and incubated for 24 h at 37°C under aerobic condition. The colonies were counted, and data were expressed as the $\log_{10}$ of colony-forming units (CFU) per milligram of feces. *Enterobacteriaceae* colonies with different morphologies were isolated from MacConkey agar. Pure colonies were suspended in sterile 0.9% saline at a $1.5x10^8$ CFU/mL concentration according to the 0.5 McFarland standard. Then, a sterile swab was soaked in the bacterium solution and inoculated by spreading on Mueller Hinton Agar plates (140x15 mm) (Merck, USA). After 15 minutes, a dispenser (Thermo Scientific, Remel™, USA) with 12 discs (Thermo Scientific, Oxoid™, USA) referring to β-lactam (amoxicillin-clavulanic acid, cephalosporin, ertapenem, meropenem, imipenem), aminoglycosides (amikacin, streptomycin, gentamicin), quinolones (ciprofloxacin, levofloxacin, norfloxacin), sulfonamide and folate inhibitors (sulfamethoxazole-trimethoprim) and macrolides (azithromycin) antibiotics were added to the inoculated plates. The plates were incubated at 37°C for 24 h. The presence or absence of bacterial growth inhibition zones was observed and measured to determine the resistance profile in: sensitive, intermediate, or resistant, according to the CLSI M100Ed31 guidelines. The resistance phenotype was determined according to the number of antimicrobial classes in which each strain presented resistance, being resistant (1-2 antimicrobials) or multidrug-resistant (≥3 antimicrobials). Identification of *Enterobacteriaceae* strains was performed by Matrix Associated Laser Desorption-Ionization - Time of Flight (MALDI-TOF), using the FlexControl MicroFlex LT mass spectrometer (Brunker Daltonics, USA) as described before (Assis et al., 2017). Before identification, calibration was done with the bacteria *Escherichia coli* DH5α test standard (Brunker Daltonics, USA).

Laboratory animals

Male and female germ-free Swiss/NIH mice derived from a GF nucleus (Taconic Farms, USA), with ~8-weeks-old were used. They were maintained in flexible plastic isolators (Standard Safety Equipment Co., USA) using classical gnotobiology techniques at the Gnotobiology Laboratory of the Federal University of Minas Gerais (UFMG), Minas Gerais, Brazil and with controlled conditions (26°C, 12h light/dark

cycle). For FMT experiments, each germ-free mouse was kept individually in sterile microisolator cage (UNO Roestvaststaal B.V., Netherlands) throughout the experiment, to avoid cross-contamination and ensure the individual feces donor phenotype for the respective HM mice. Also, male and female C57BL/6J mice, aging ~8 weeks old, obtained from the UFMG animal facility, were kept in plastic cages (Alesco, Monte Mor, Brazil) in a room with controlled conditions (26°C, 12h light/dark cycle) with steam sterilized food (Nuvilab, Brazil) and sterile water *ad libitum*. All mouse procedures were performed in accordance with guidelines from the Guide for the Care and Use of Laboratory Animals of the Brazilian National Council of Animal Experimentation (http://www.cobea.org.br/) and Brazilian Federal Law 11.794 (October 8, 2008). The animal study was reviewed and approved by The Institutional Committee for Animal Ethics of the Federal University of Minas Gerais (protocol nº CEUA/UFMG 281/2020 and 55/2021).

Human fecal microbiota transplant to GF mice

Fresh fecal samples were used for the FMT and samples from members of the same household were prioritized (n=6 families; in total n=12 members). In addition, randomized samples of post-COVID subjects were included (n=8), totaling n=19 samples (Figure 2—figure supplement 1F). Each sample was weighed and resuspended (100 mg/mL) in 0.9% sterile saline (NaCl) solution. The FMT was performed individually, in which each animal received a sample from an individual donor volunteer. A 100 µL aliquot was used for oral gavage of GF mice, with the same concentration and volume of feces/bacteria in all the animals. After nine days, the experiments were performed to ensure a stable human microbiota population of GF mice when we were able to transfer human bacteria to GF mice according with previously from our group (Souza et al., 2004; Angélica T Vieira et al., 2015).

Histopathology and immunohistochemistry

Intestine and lung tissue from HM mice were collected and processed. For the intestinal morphometric analysis, the images (20X objective) were acquired from H&E stained for quantification of the colonic lymphoid patches and globet cells, we counted the absolute number of colon globet cells per epithelial ratio and perimeter of lymphoid patches in the controls compared to post-COVID mice. For the lung analysis, inflammatory score was performed with hematoxylin and eosin (H&E)

stained slides and evaluated airway, vascular and parenchymal inflammation, as previously described (Garcia et al., 2010; Horvat et al., 2007). For immunohistochemistry analysis, lung tissue slides from controls and post-COVID HM mice were immune-stained. Briefly, the slides were incubated with primary anti-α-actin antibodies (human, 1:500) (DAKO, USA) overnight at 4ºC. Then, the primary antibodies were detected using an anti-mouse/anti-rabbit detection system (Novolink Polymer Detection System; Leica Biosystems, UK) according to the manufacturer's instructions. The sections were counterstained in diluted Harris Hematoxylin solution and permanently mounted with Entellan (Merck, USA). For the morphometric analysis, images (20X objective) were acquired from α-actin immunolabeled to quantify the muscle layer of the lung section. For intestine and lung morphometric analysis, we used the Image J 1.52 program (NIH, USA). All the analyses were examined under a light microscope by a pathologist who was blinded to the experiment.

Bronchoalveolar lavage collection and analysis

After anesthetizing and euthanizing the mice (ketamine/xylazine - 180 and 12 mg/kg, respectively), bronchoalveolar lavage (BAL) was performed by inserting and collecting 1 mL of sterile phosphate-buffered saline (PBS) through a 20-gauge catheter in a 1-mL syringe. The *Enterobacteriaceae* quantification was performed by plating an aliquot (100 µL) in MacConkey medium and incubated in aerobic conditions for 24 h and 37°C. Then the colonies count was performed and expressed in CFU per mL of BAL. For airway inflammatory cell counts, the remaining BAL was centrifuged, resuspended in 100 µL of saline, and total leukocytes were quantified by Neubauer chamber counting.

***Klebsiella pneumoniae* infection**

K. pneumoniae B31, a clinical isolate with an AMR profile (Profeta et al., 2021), was kindly provided by Prof. Vasco Azevedo, Laboratory of Cellular and Molecular Genetics at ICB/UFMG. Intratracheal infection was performed as previously described (Vieira et al., 2016b). Briefly, with anesthetized animals the trachea was exposed and 25 µL of the suspension containing 1×10^6 CFU/mL of *K. pneumoniae* B31, or sterile saline for vehicle control animals, was administered with a 26-gauge needle.

Short-chain fatty acid (SCFA) assays

Human and mouse fecal samples were suspended in 1% phosphoric acid (1:6 weight:volume) (Merck, USA), vortexed, and centrifuged (20,000x*g*, 30 min, 4°C). Supernatants were filtered (0.22 µm) and injected directly into an HPLC, with an ionic exchange resin column 300×7.8 mm (Sigma, Germany) at 30ºC with a Micro-Guard cation H^+ cartridge (Sigma, Germany) and detector set at 210 nm. The flow rate was 0.5 mL/min for 35 minutes, changed to 0.7 mL/min until the end of the 55 minutes of chromatographic runs. Serum samples were diluted in formic acid (1 $mol.L^{-1}$), and internal standard, 2-ethyl-butyric acid 1 $mol.L^{-1}$, (Sigma, Germany) was added, in proportions 5:5:1 respectively, followed by vortexing and centrifugation (12,000x*g*, 30 min, 4°C). Next, supernatants were injected into a Gas Chromatograph–FID (Agilent, USA), with an HP-FFAP column 19091F-105 (Agilent, USA), 50m×0.20mm×0.33 µm, and the detector set at 240°C. Chromatographic conditions were 60°C for 0.5 minutes, heating at 8°C.min^{-1} to 180°C for 1 minute, with a new heating rate from 20 °C.min^{-1} to 240 °C for 7 minutes. Total run time was 26.5 minutes. Seven-point external calibration curves were adopted to quantify fecal and serum samples, using analytical grade SCFA (Sigma, Germany) as standards.

Mouse behavioral tests

Tests were performed in a 30 (w) x 30 (d) x 45 (h) cm arena, where each animal was allowed to freely explore for 5 min. On the next day, mice were subjected to a 5 min training session during which animals were placed at the center of the arena in the presence of two identical objects, and the time spent exploring each object was recorded. The test session was performed after 30 minutes by replacing one of the two identical objects with a new one in the object recognition paradigm, or moving the training object to a new location in the new object location paradigm (Melo et al., 2020). Results were expressed as a percentage of time exploring each object or location, old (O) or new (N) in relation to the total exploration time during the test session.

Mouse hippocampus analysis

Total RNA of the hippocampus from post-COVID HM mice and controls was extracted using TRIzol™ reagent (Thermo Scientific, USA). cDNAs were synthesized and subjected to qPCR using Power SYBR Green Master Mix kits following the

597 manufacturer's instructions in the QuantStudio™ 7 Flex real-time PCR system
598 platform (Applied Biosystems, USA). Primer sequences used are described in Table
599 3. Gene expression changes were determined by the $2^{-\Delta Ct}$ method using Ribosomal
600 protein L32 for normalization.

601 **Mouse Hepatitis Virus-3 (MHV-3) infection**

602 The β-coronavirus mouse hepatitis virus MHV-3 (3×10^1 PFU), propagated in
603 L929 cells, or sterile saline for sham controls, was used to intranasally infect
604 C57BL/6J mice as previously described (Andrade et al., 2021). Some groups were
605 treated with B. longum 5^{1A}. The probiotic bacterium *B. longum* 5^{1A}*,* from the culture
606 collection of the Laboratory of Biotherapeutic Agents at ICB/UFMG, was isolated
607 from fecal samples of healthy children and was cultivated as previously described
608 (Santos et al., 2021; Vieira et al., 2016b). Briefly, mice were treated by oral gavage
609 of a single 100 µL dose of suspension containing $1x10^9$ CFU/mL *B. longum* 5^{1A}, or
610 sterile saline every 48h during the infection period (Vieira et al., 2016b). Four days
611 after infection, behavioral tests were performed.

612 **Intestinal fatty acid-binding protein (I-FABP) assays**

613 The I-FABP were quantified by enzyme-linked immunosorbent assay in
614 accordance to the manufacturer's instructions (R&D Systems, USA) and as
615 previously described (Saia et al., 2021).

616 **Statistical analysis**

617 Statistical analyses were produced using GraphPad Prism7 (GraphPad
618 Software, USA) and R software v.4.2.2 (R Core Team, 2013). The graphs were
619 produced GraphPad Prism7 e Microsoft PowerBi (Microsoft Corporation, USA). Data
620 normality and homoscedasticity were tested using the Shapiro-Wilk and Levene test,
621 respectively. Data with a normal distribution were evaluated by Student's *t* test
622 paired or unpaired, one-way or two-way analysis of variance (ANOVA). Following
623 significant ANOVAs, the post-hoc test was performed according to the coefficient of
624 variation (CV): Tukey (CV ≤ 15%), Student's Newman-Keuls (CV 15-30%) e Duncan
625 (CV >30%). Non-parametric tests were applied to data that did not show normal
626 distribution, Mann-Whitney or Kruskal-Wallis e post-hoc of Dunn's. For categorical
627 data were applied Fisher's exact test, Chi-square test or Wald test, depending on the
628 experimental design. Data are shown as mean ± standard deviation (SD).

Consent for publication

Not applicable.

Data availability

The 16S rRNA gene libraries produced in this work were deposited in the NCBI SRA database under project number PRJNA843134. Data are available upon appropriate request to the corresponding author.

Competing interests

All authors declare no conflict of interest.

Funding

This work was supported by National Council for Scientific and Technological Development – CNPq (call MCTIC/CNPq/FNDCT/MS/SCTIE/Decit 07/2020 [process number: 402530/2020-9], Universal MCTIC/CNPq [process number: 408703/2021-0]), Fundação de Amparo à Pesquisa de Minas Gerais (FAPEMIG) (APQ-03328-18; APQ-00686-21), and Instituto Serrapilheira (Nº 03/2019): A.T.V.
Coordenação de Aperfeiçoamento de Pessoal de Nível Superior, Brazil (CAPES) Finance Code 001: V.M.A and D.A.A.
CAPES-Print: I.G.
Pró-Reitoria de Pesquisa da Universidade Federal de Minas Gerais – PRPq:
São Paulo Research Foundation (grants 2017/25588-1, 2018/14666-4, 2019/00098-7, 2019/05155-9 and 2020/04746-0): R.S.S. and D.M.S.
National Health and Medical Research Council of Australia (105,9238, 1175134, 2010287): P.M.M.

Contributors

Study conception, methodology, supervision, project administration and funding acquisition: A.T.V.
Investigation: V.M., D.F.E., M.F.R., C.S.C., D.A.A., M.A., J.M., E.C.M., V.M.R., T.G.C., L.S.B.L., J.C.P., M.A., G.S.Z., B.J.S., V.C.C., E.S.R., I.G., and C.C.G.
Formal analysis and interpretation of data: V.M., M.F.R., D.F.E., C.S.C., E.R.G.R.A, I.S.L., D.A.A., T.G.C., G.D.C., and D.M.S,
Data curation: V.M., E.R.G.R.A, and I.S.L.

Resources: F.S.M., J.T.M., F.M.R., L.C.A., M.M.T., V.V.C., R.S.S.
Writing—original draft: V.M., A.T.V., M.F.R., and D.F.E.
Writing—review & editing: J.T.M., P.M.H., M.M.T., and A.T.V.
Visualization: V.M., C.S.C. A.T.V., and M.F.R.

Acknowledgments

Prof. Vasco Azevedo for providing the *K. pneumonia* B31 clinical isolate; Prof. Vivian Vasconcelos Costa and Prof. Mauro Martins Teixeira for providing the mouse hepatitis virus MHV-3; Prof. Flaviano S. Martins for providing the probiotic strain *B. longum* 5^{1A}. Daniela M. Nolasco and Prof. Leda Quercia Vieira for technical support; Eduardo Zimmer, Andreza F. de Bem, and Ana Maria Caetano de Faria for valuable discussions.

References

Al Bataineh MT, Henschel A, Mousa M, Daou M, Waasia F, Kannout H, Khalili M, Kayasseh MA, Alkhajeh A, Uddin M. 2021. Gut microbiota interplay with COVID-19 reveals links to host lipid metabolism among Middle Eastern populations. *Front Microbiol* **12**. doi: 10.3389/fmicb.2021.761067

Alharbi KS, Singh Y, Hassan Almalki W, Rawat S, Afzal O, Alfawaz Altamimi AS, Kazmi I, Al-Abbasi FA, Alzarea SI, Singh SK, Bhatt S, Chellappan DK, Dua K, Gupta G. 2022. Gut Microbiota Disruption in COVID-19 or Post-COVID Illness Association with severity biomarkers: A Possible Role of Pre / Pro-biotics in manipulating microflora. *Chem Biol Interact* **358**:109898. doi:10.1016/j.cbi.2022.109898

Andrade AC dos SP, Campolina-Silva GH, Queiroz-Junior CM, de Oliveira LC, Lacerda L de SB, Gaggino JCP, de Souza FRO, de Meira Chaves I, Passos IB, Teixeira DC, Bittencourt-Silva PG, Valadão PAC, Rossi-Oliveira L, Antunes MM, Figueiredo AFA, Wnuk NT, Temerozo JR, Ferreira AC, Cramer A, Oliveira CA, Durães-Carvalho R, Weis Arns C, Guimarães PPG, Costa GMJ, de Menezes GB, Guatimosim C, da Silva GSF, Souza TML, Barrioni BR, Pereira M de M, de Sousa LP, Teixeira MM, Costa VV. 2021. A Biosafety Level 2 Mouse Model for Studying Betacoronavirus-Induced Acute Lung Damage and Systemic Manifestations. *J Virol* **95**. doi:10.1128/JVI.01276-21

691 Arcari G, Raponi G, Sacco F, Bibbolino G, Di Lella FM, Alessandri F, Coletti M,
692 Trancassini M, Deales A, Pugliese F, Antonelli G, Carattoli A. 2021. Klebsiella
693 pneumoniae infections in COVID-19 patients: a 2-month retrospective analysis
694 in an Italian hospital. *Int J Antimicrob Agents*.
695 doi:10.1016/j.ijantimicag.2020.106245

696 Assis GBN, Pereira FL, Zegarra AU, Tavares GC, Leal CA, Figueiredo HCP. 2017.
697 Use of MALDI-TOF Mass Spectrometry for the Fast Identification of Gram-
698 Positive Fish Pathogens. *Front Microbiol* **8**. doi:10.3389/fmicb.2017.01492

699 Augustin M, Schommers P, Stecher M, Dewald F, Gieselmann L, Gruell H, Horn C,
700 Vanshylla K, Di Cristanziano V, Osebold L. 2021. Post-COVID syndrome in non-
701 hospitalised patients with COVID-19: a longitudinal prospective cohort study.
702 *Lancet Reg Heal* **6**:100122. doi: 10.1016/j.lanepe.2021.100122

703 Bajinka O, Simbilyabo L, Tan Y, Jabang J, Saleem SA. 2022. Lung-brain axis. *Crit*
704 *Rev Microbiol* **48**:257–269. doi:10.1080/1040841X.2021.1960483

705 Bazaid AS, Barnawi H, Qanash H, Alsaif G, Aldarhami A, Gattan H, Alharbi B,
706 Alrashidi A, Al-Soud WA, Moussa S, Alfouzan F. 2022. Bacterial Coinfection and
707 Antibiotic Resistance Profiles among Hospitalised COVID-19 Patients.
708 *Microorganisms* **10**:495. doi:10.3390/microorganisms10030495

709 Bernard-Raichon L, Venzon M, Klein J, Axelrad JE, Zhang C, Sullivan AP, Hussey
710 GA, Casanovas-Massana A, Noval MG, Valero-Jimenez AM, Gago J, Putzel G,
711 Pironti A, Wilder E, Obaid A, Lu-Culligan A, Nelson A, Brito A, Nunez A, Martin
712 A, Watkins A, Geng B, Kalinich C, Harden C, Todeasa C, Jensen C, Kim D,
713 McDonald D, Shepard D, Courchaine E, White EB, Song E, Silva E, Kudo E,
714 Deluliis G, Rahming H, Park H-J, Matos I, Nouws J, Valdez J, Fauver J, Lim J,
715 Rose K-A, Anastasio K, Brower K, Glick L, Sharma L, Sewanan L, Knaggs L,
716 Minasyan M, Batsu M, Petrone M, Kuang M, Nakahata M, Campbell M, Linehan
717 M, Askenase MH, Simonov M, Smolgovsky M, Sonnert N, Naushad N,
718 Vijayakumar P, Martinello R, Datta R, Handoko R, Bermejo S, Prophet S,
719 Bickerton S, Velazquez S, Alpert T, Rice T, Khoury-Hanold W, Peng X, Yang Y,
720 Cao Y, Strong Y, Thorpe LE, Littman DR, Dittmann M, Stapleford KA, Shopsin
721 B, Torres VJ, Ko AI, Iwasaki A, Cadwell K, Schluter J, Team YIR. 2022. Gut

722 microbiome dysbiosis in antibiotic-treated COVID-19 patients is associated with
723 microbial translocation and bacteremia. *Nat Commun* **13**:5926.
724 doi:10.1038/s41467-022-33395-6

725 Blighe, Kevin, Sharmila Rana and ML. 2019. “EnhancedVolcano: Publication-ready
726 volcano plots with enhanced colouring and labeling.” *R Packag version 1* **no. 0**.

727 Bolyen E, Rideout JR, Dillon MR, Bokulich NA, Abnet CC, Al-Ghalith GA, Alexander
728 H, Alm EJ, Arumugam M, Asnicar F, Bai Y, Bisanz JE, Bittinger K, Brejnrod A,
729 Brislawn CJ, Brown CT, Callahan BJ, Caraballo-Rodríguez AM, Chase J, Cope
730 EK, Da Silva R, Diener C, Dorrestein PC, Douglas GM, Durall DM, Duvallet C,
731 Edwardson CF, Ernst M, Estaki M, Fouquier J, Gauglitz JM, Gibbons SM,
732 Gibson DL, Gonzalez A, Gorlick K, Guo J, Hillmann B, Holmes S, Holste H,
733 Huttenhower C, Huttley GA, Janssen S, Jarmusch AK, Jiang L, Kaehler BD,
734 Kang K Bin, Keefe CR, Keim P, Kelley ST, Knights D, Koester I, Kosciolek T,
735 Kreps J, Langille MGI, Lee J, Ley R, Liu Y-X, Loftfield E, Lozupone C, Maher M,
736 Marotz C, Martin BD, McDonald D, McIver LJ, Melnik A V., Metcalf JL, Morgan
737 SC, Morton JT, Naimey AT, Navas-Molina JA, Nothias LF, Orchanian SB,
738 Pearson T, Peoples SL, Petras D, Preuss ML, Pruesse E, Rasmussen LB,
739 Rivers A, Robeson MS, Rosenthal P, Segata N, Shaffer M, Shiffer A, Sinha R,
740 Song SJ, Spear JR, Swafford AD, Thompson LR, Torres PJ, Trinh P, Tripathi A,
741 Turnbaugh PJ, Ul-Hasan S, van der Hooft JJJ, Vargas F, Vázquez-Baeza Y,
742 Vogtmann E, von Hippel M, Walters W, Wan Y, Wang M, Warren J, Weber KC,
743 Williamson CHD, Willis AD, Xu ZZ, Zaneveld JR, Zhang Y, Zhu Q, Knight R,
744 Caporaso JG. 2019. Reproducible, interactive, scalable and extensible
745 microbiome data science using QIIME 2. *Nat Biotechnol* **37**:852–857.
746 doi:10.1038/s41587-019-0209-9

747 Bowermicrobiomeman KL, Rehman SF, Vaughan A, Lachner N, Budden KF, Kim
748 RY, Wood DLA, Gellatly SL, Shukla SD, Wood LG, Yang IA, Wark PA,
749 Hugenholtz P, Hansbro PM. 2020. Disease-associated gut and metabolome
750 changes in patients with chronic obstructive pulmonary disease. *Nat Commun*
751 **11**:5886. doi:10.1038/s41467-020-19701-0

752 Caugant DA, Levin BR, Selander RK. 1984. Distribution of multilocus genotypes of

753 Escherichia coli within and between host families. *J Hyg (Lond)* **92**:377–384.
754 doi:10.1017/S0022172400064597

755 Chen Yanfei, Gu S, Chen Yunbo, Lu H, Shi D, Guo J, Wu W-R, Yang Y, Li Y, Xu K-
756 J, Ding C, Luo R, Huang C, Yu L, Xu M, Yi P, Liu J, Tao J, Zhang H, Lv L, Wang
757 B, Sheng J, Li L. 2022. Six-month follow-up of gut microbiota richness in
758 patients with COVID-19. *Gut* **71**:222–225. doi:10.1136/gutjnl-2021-324090

759 Chong WH, Saha BK, Ananthakrishnan Ramani, Chopra A. 2021. State-of-the-art
760 review of secondary pulmonary infections in patients with COVID-19
761 pneumonia. *Infection* **49**:591–605. doi:10.1007/s15010-021-01602-z

762 Coryell MP, Iakiviak M, Pereira N, Murugkar PP, Rippe J, Williams DB, Heald-
763 Sargent T, Sanchez-Pinto LN, Chavez J, Hastie JL, Sava RL, Lien CZ, Wang
764 TT, Muller WJ, Fischbach MA, Carlson PE. 2021. A method for detection of
765 SARS-CoV-2 RNA in healthy human stool: a validation study. *The Lancet*
766 *Microbe* **2**:e259–e266. doi:10.1016/S2666-5247(21)00059-8

767 Cullen BR. 2013. MicroRNAs as mediators of viral evasion of the immune system.
768 *Nat Immunol* **14**:205–10. doi:10.1038/ni.2537

769 da Silva JGV, Vieira AT, Sousa TJ, Viana MVC, Parise D, Sampaio B, da Silva AL,
770 de Jesus LCL, de Carvalho PKRML, de Castro Oliveira L, Aburjaile FF, Martins
771 FS, Nicoli JR, Ghosh P, Brenig B, Azevedo V, Gomide ACP. 2021. Comparative
772 genomics and in silico gene evaluation involved in the probiotic potential of
773 Bifidobacterium longum 51A. *Gene* **795**:145781.
774 doi:10.1016/j.gene.2021.145781

775 Dang AT, Marsland BJ. 2019. Microbes, metabolites, and the gut–lung axis. *Mucosal*
776 *Immunol* **12**:843–850. doi:10.1038/s41385-019-0160-6

777 de Nies L, Galata V, Martin-Gallausiaux C, Despotovic M, Busi SB, Snoeck CJ,
778 Delacour L, Budagavi DP, Laczny CC, Habier J, Lupu P-C, Halder R, Fritz J V,
779 Marques T, Sandt E, O'Sullivan MP, Ghosh S, Satagopam V, Krüger R,
780 Fagherazzi G, Ollert M, Hefeng FQ, May P, Wilmes P. 2023. Altered infective
781 competence of the human gut microbiome in COVID-19. *Microbiome* **11**:46.

782 doi:10.1186/s40168-023-01472-7

783 Doifode T, Giridharan V V., Generoso JS, Bhatti G, Collodel A, Schulz PE, Forlenza
784 O V., Barichello T. 2021. The impact of the microbiota-gut-brain axis on
785 Alzheimer's disease pathophysiology. *Pharmacol Res* **164**:105314.
786 doi:10.1016/j.phrs.2020.105314

787 Douaud G, Lee S, Alfaro-Almagro F, Arthofer C, Wang C, McCarthy P, Lange F,
788 Andersson JLR, Griffanti L, Duff E. 2022. SARS-CoV-2 is associated with
789 changes in brain structure in UK Biobank. *Nature* **604**:697–707.

790 Erny D, Hrabě de Angelis AL, Jaitin D, Wieghofer P, Staszewski O, David E, Keren-
791 Shaul H, Mahlakoiv T, Jakobshagen K, Buch T, Schwierzeck V, Utermöhlen O,
792 Chun E, Garrett WS, McCoy KD, Diefenbach A, Staeheli P, Stecher B, Amit I,
793 Prinz M. 2015. Host microbiota constantly control maturation and function of
794 microglia in the CNS. *Nat Neurosci* **18**:965–77. doi:10.1038/nn.4030

795 Fernández-de-Las-Peñas C, Palacios-Ceña D, Gómez-Mayordomo V, Cuadrado
796 ML, Florencio LL. 2021. Defining Post-COVID Symptoms (Post-Acute COVID,
797 Long COVID, Persistent Post-COVID): An Integrative Classification. *Int J*
798 *Environ Res Public Health* **18**. doi:10.3390/ijerph18052621

799 Furlan L, Caramelli B. 2021. The regrettable story of the "Covid Kit" and the "Early
800 Treatment of Covid-19" in Brazil. *Lancet Reg Heal - Am* **4**:100089.
801 doi:10.1016/j.lana.2021.100089

802 Galvão I, Tavares LP, Corrêa RO, Fachi JL, Rocha VM, Rungue M, Garcia CC,
803 Cassali G, Ferreira CM, Martins FS, Oliveira SC, Mackay CR, Teixeira MM,
804 Vinolo MAR, Vieira AT. 2018. The Metabolic Sensor GPR43 Receptor Plays a
805 Role in the Control of Klebsiella pneumoniae Infection in the Lung. *Front*
806 *Immunol* **9**. doi:10.3389/fimmu.2018.00142

807 Garcia CC, Russo RC, Guabiraba R, Fagundes CT, Polidoro RB, Tavares LP,
808 Salgado APC, Cassali GD, Sousa LP, Machado A V., Teixeira MM. 2010.
809 Platelet-Activating Factor Receptor Plays a Role in Lung Injury and Death
810 Caused by Influenza A in Mice. *PLoS Pathog* **6**:e1001171.

811 doi:10.1371/journal.ppat.1001171

812 Gerver SM, Guy R, Wilson K, Thelwall S, Nsonwu O, Rooney G, Brown CS, Muller-
813 Pebody B, Hope R, Hall V. 2021. National surveillance of bacterial and fungal
814 coinfection and secondary infection in COVID-19 patients in England: lessons
815 from the first wave. *Clin Microbiol Infect* **27**:1658–1665.
816 doi:https://doi.org/10.1016/j.cmi.2021.05.040

817 Hartung TJ, Neumann C, Bahmer T, Chaplinskaya-Sobol I, Endres M, Geritz J,
818 Haeusler KG, Heuschmann PU, Hildesheim H, Hinz A. 2022. Fatigue and
819 cognitive impairment after COVID-19: A prospective multicentre study.
820 *EClinicalMedicine* **53**:101651. doi: 10.1016/j.eclinm.2022.101651

821 Heine J, Schwichtenberg K, Hartung TJ, Rekers S, Chien C, Boesl F, Rust R,
822 Hohenfeld C, Bungenberg J, Costa AS. 2023. Structural brain changes in
823 patients with post-COVID fatigue: a prospective observational study.
824 *Eclinicalmedicine* **58**. doi: 10.1016/j.eclinm.2023

825 Hikmet F, Méar L, Edvinsson Å, Micke P, Uhlén M, Lindskog C. 2020. The protein
826 expression profile of ACE2 in human tissues. *Mol Syst Biol* **16**:e9610.
827 doi:10.15252/msb.20209610

828 Horvat JC, Beagley KW, Wade MA, Preston JA, Hansbro NG, Hickey DK, Kaiko GE,
829 Gibson PG, Foster PS, Hansbro PM. 2007. Neonatal Chlamydial Infection
830 Induces Mixed T-Cell Responses That Drive Allergic Airway Disease. *Am J*
831 *Respir Crit Care Med* **176**:556–564. doi:10.1164/rccm.200607-1005OC

832 Hosang L, Canals RC, van der Flier FJ, Hollensteiner J, Daniel R, Flügel A, Odoardi
833 F. 2022. The lung microbiome regulates brain autoimmunity. *Nature* **603**:138–
834 144. doi:10.1038/s41586-022-04427-4

835 Jang S-E, Lim S-M, Jeong J-J, Jang H-M, Lee H-J, Han MJ, Kim D-H. 2018.
836 Gastrointestinal inflammation by gut microbiota disturbance induces memory
837 impairment in mice. *Mucosal Immunol* **11**:369–379. doi:10.1038/mi.2017.49

838 Jang YO, Kim O-H, Kim SJ, Lee SH, Yun S, Lim SE, Yoo HJ, Shin Y, Lee SW. 2021.
839 High-fiber diets attenuate emphysema development via modulation of gut

microbiota and metabolism. *Sci Rep* **11**:7008. doi:10.1038/s41598-021-86404-x

Jeon K, Jeong S, Lee N, Park M-J, Song W, Kim H-S, Kim HS, Kim J-S. 2022. Impact of COVID-19 on Antimicrobial Consumption and Spread of Multidrug-Resistance in Bacterial Infections. *Antibiotics*. doi:10.3390/antibiotics11040535

Johansen MD, Mahbub RM, Idrees S, Nguyen DH, Miemczyk S, Pathinayake P, Nichol K, Hansbro NG, Gearing LJ, Hertzog PJ, Gallego-Ortega D, Britton WJ, Saunders BM, Wark PA, Faiz A, Hansbro PM. 2022. Increased SARS-CoV-2 Infection, Protease and Inflammatory Responses in COPD Primary Bronchial Epithelial Cells Defined with Single Cell RNA-Sequencing. *Am J Respir Crit Care Med*. doi:10.1164/rccm.202108-1901OC

Karami Z, Knoop BT, Dofferhoff ASM, Blaauw MJT, Janssen NA, van Apeldoorn M, Kerckhoffs APM, van de Maat JS, Hoogerwerf JJ, ten Oever J. 2021. Few bacterial co-infections but frequent empiric antibiotic use in the early phase of hospitalized patients with COVID-19: results from a multicentre retrospective cohort study in The Netherlands. *Infect Dis (Auckl)* **53**:102–110. doi:10.1080/23744235.2020.1839672

Kariyawasam RM, Julien DA, Jelinski DC, Larose SL, Rennert-May E, Conly JM, Dingle TC, Chen JZ, Tyrrell GJ, Ronksley PE, Barkema HW. 2022. Antimicrobial resistance (AMR) in COVID-19 patients: a systematic review and meta-analysis (November 2019–June 2021). *Antimicrob Resist Infect Control* **11**:45. doi:10.1186/s13756-022-01085-z

Kim N, Jeon SH, Ju IG, Gee MS, Do J, Oh MS, Lee JK. 2021. Transplantation of gut microbiota derived from Alzheimer's disease mouse model impairs memory function and neurogenesis in C57BL/6 mice. *Brain Behav Immun* **98**:357–365. doi:10.1016/j.bbi.2021.09.002

Langford BJ, So M, Simeonova M, Leung V, Lo J, Kan T, Raybardhan S, Sapin ME, Mponponsuo K, Farrell A. 2022a. Antimicrobial resistance in patients with COVID-19: a systematic review and meta-analysis. *The Lancet Microbe*. doi:10.1016/S2666-5247(22)00355-X

869 Liu Q, Mak JWY, Su Q, Yeoh YK, Lui GC-Y, Ng SSS, Zhang F, Li AYL, Lu W, Hui
870 DS-C, Chan PK, Chan FKL, Ng SC. 2022. Gut microbiota dynamics in a
871 prospective cohort of patients with post-acute COVID-19 syndrome. *Gut*
872 **71**:544–552. doi:10.1136/gutjnl-2021-325989

873 Livanos AE, Jha D, Cossarini F, Gonzalez-Reiche AS, Tokuyama M, Aydillo T, Parigi
874 TL, Ladinsky MS, Ramos I, Dunleavy K, Lee B, Dixon RE, Chen ST, Martinez-
875 Delgado G, Nagula S, Bruce EA, Ko HM, Glicksberg BS, Nadkarni G, Pujadas
876 E, Reidy J, Naymagon S, Grinspan A, Ahmad J, Tankelevich M, Bram Y,
877 Gordon R, Sharma K, Houldsworth J, Britton GJ, Chen-Liaw A, Spindler MP,
878 Plitt T, Wang P, Cerutti A, Faith JJ, Colombel J-F, Kenigsberg E, Argmann C,
879 Merad M, Gnjatic S, Harpaz N, Danese S, Cordon-Cardo C, Rahman A,
880 Schwartz RE, Kumta NA, Aghemo A, Bjorkman PJ, Petralia F, van Bakel H,
881 Garcia-Sastre A, Mehandru S. 2021. Intestinal Host Response to SARS-CoV-2
882 Infection and COVID-19 Outcomes in Patients With Gastrointestinal Symptoms.
883 *Gastroenterology* **160**:2435-2450.e34. doi:10.1053/j.gastro.2021.02.056

884 López-Jácome LE, Fernández-Rodríguez D, Franco-Cendejas R, Camacho-Ortiz A,
885 Morfin-Otero MDR, Rodríguez-Noriega E, Ponce-de-León A, Ortiz-Brizuela E,
886 Rojas-Larios F, Velázquez-Acosta MDC, Mena-Ramírez JP, Rodríguez-Zulueta
887 P, Bolado-Martínez E, Quintanilla-Cazares LJ, Avilés-Benítez LK, Consuelo-
888 Munoz S, Choy-Chang EV, Feliciano-Guzmán JM, Couoh-May CA, López-
889 Gutiérrez E, Molina-Jaimes A, Rincón-Zuno J, Gil-Veloz M, Alcaraz-Espejel M,
890 Corte-Rojas RE, Gómez-Espinosa J, Monroy-Colin VA, Morales-de-la-Peña CT,
891 Aguirre-Burciaga E, López-Moreno LI, Martínez-Villarreal RT, Cetina-Umaña
892 CM, Galindo-Méndez M, Soto-Nieto GI, Cobos-Canul DI, Moreno-Méndez MI,
893 Tello-Gómez E, Romero-Romero D, Quintana-Ponce S, Peralta-Catalán R,
894 Valadez-Quiroz A, Molina-Chavarría A, Padilla-Ibarra C, Barroso-Herrera-Y-
895 Cairo IE, Duarte-Miranda LS, López-López DM, Escalante-Armenta SP, Osorio-
896 Guzmán MJ, López-García M, Garza-Ramos U, Delgado-Enciso I, Garza-
897 González E. 2022. Increment Antimicrobial Resistance During the COVID-19
898 Pandemic: Results from the Invifar Network. *Microb Drug Resist* **28**:338–345.
899 doi:10.1089/mdr.2021.0231

900 Lopez-Leon S, Wegman-Ostrosky T, Perelman C, Sepulveda R, Rebolledo PA,

Cuapio A, Villapol S. 2021. More than 50 long-term effects of COVID-19: a systematic review and meta-analysis. *Sci Rep* **11**:16144. doi:10.1038/s41598-021-95565-8

Love M, Anders S, Huber W. 2014. Differential analysis of count data–the DESeq2 package. *Genome Biol* **15**:10–1186.

Lu Z-H, Zhou H-W, Wu W-K, Fu T, Yan M, He Z, Sun S-W, Ji Z-H, Shao Z. 2021. Alterations in the Composition of Intestinal DNA Virome in Patients With COVID-19 . *Front Cell Infect Microbiol* . doi: 10.3389/fcimb.2021.790422

M C C C, N L L, C M F, J L G, D A, C G, G C, S H P, C M, F S M, J R N, M M T, A L B G, A T V. 2014. Comparing the effects of acute alcohol consumption in germ-free and conventional mice: the role of the gut microbiota. *BMC Microbiol* **14**:240. doi:10.1186/s12866-014-0240-4

Mańkowska-Wierzbicka D, Zuraszek J, Wierzbicka A, Gabryel M, Mahadea D, Baturo A, Zakerska-Banaszak O, Slomski R, Skrzypczak-Zielinska M, Dobrowolska A. 2023. Alterations in Gut Microbiota Composition in Patients with COVID-19: A Pilot Study of Whole Hypervariable 16S rRNA Gene Sequencing. *Biomedicines* **11**. doi:10.3390/biomedicines11020367

Melo HM, Seixas da Silva G da S, Sant'Ana MR, Teixeira CVL, Clarke JR, Miya Coreixas VS, de Melo BC, Fortuna JTS, Forny-Germano L, Ledo JH, Oliveira MS, Figueiredo CP, Pardossi-Piquard R, Checler F, Delgado-García JM, Gruart A, Velloso LA, Balthazar MLF, Cintra DE, Ferreira ST, De Felice FG. 2020. Palmitate Is Increased in the Cerebrospinal Fluid of Humans with Obesity and Induces Memory Impairment in Mice via Pro-inflammatory TNF-α. *Cell Rep* **30**:2180-2194.e8. doi:10.1016/j.celrep.2020.01.072

Merad M, Blish CA, Sallusto F, Iwasaki A. 2022. The immunology and immunopathology of COVID-19. *Science (80-)* **375**:1122–1127. doi:10.1126/science.abm8108

Monje M, Iwasaki A. 2022. The Neurobiology of Long COVID. *Neuron*. doi:https://doi.org/10.1016/j.neuron.2022.10.006

930 Mukhopadhya I, Segal JP, Carding SR, Hart AL, Hold GL. 2019. The gut virome: the
931 “missing link” between gut bacteria and host immunity? *Therap Adv*
932 *Gastroenterol* **12**:1756284819836620. doi:10.1177/1756284819836620

933 Natarajan A, Zlitni S, Brooks EF, Vance SE, Dahlen A, Hedlin H, Park RM, Han A,
934 Schmidtke DT, Verma R, Jacobson KB, Parsonnet J, Bonilla HF, Singh U,
935 Pinsky BA, Andrews JR, Jagannathan P, Bhatt AS. 2022. Gastrointestinal
936 symptoms and fecal shedding of SARS-CoV-2 RNA suggest prolonged
937 gastrointestinal infection. *Med*. doi:10.1016/j.medj.2022.04.001

938 Pedroso SHSP, Vieira AT, Bastos RW, Oliveira JS, Cartelle CT, Arantes RME,
939 Soares PMG, Generoso S V, Cardoso VN, Teixeira MM, Nicoli JR, Martins FS.
940 2015. Evaluation of mucositis induced by irinotecan after microbial colonization
941 in germ-free mice. *Microbiology* **161**:1950–1960. doi:10.1099/mic.0.000149

942 Profeta R, Seyffert N, Tiwari S, Viana MVC, Jaiswal AK, Caetano AC, Bücker DH,
943 Tavares de Oliveira L, Santos R, Gala-Garcia A, Kato RB, Padilha FF, Lima-
944 Verde IB, Ghosh P, Barh D, Góes-Neto A, Figueiredo HCP, Soares SC, Meyer
945 R, Brenig B, Ramos PIP, Azevedo V, Castro TLP. 2021. Comparative genomics
946 with a multidrug-resistant Klebsiella pneumoniae isolate reveals the panorama
947 of unexplored diversity in Northeast Brazil. *Gene* **772**:145386.
948 doi:10.1016/j.gene.2020.145386

949 Protonotariou E, Mantzana P, Meletis G, Tychala A, Kassomenaki A, Vasilaki O,
950 Kagkalou G, Gkeka I, Archonti M, Kati S, Metallidis S, Skoura L. 2022.
951 Microbiological characteristics of bacteremias among COVID-19 hospitalized
952 patients in a tertiary referral hospital in Northern Greece during the second
953 epidemic wave. *FEMS Microbes* **2**. doi:10.1093/femsmc/xtab021

954 Quast C, Pruesse E, Yilmaz P, Gerken J, Schweer T, Yarza P, Peplies J, Glöckner
955 FO. 2012. The SILVA ribosomal RNA gene database project: improved data
956 processing and web-based tools. *Nucleic Acids Res* **41**:D590–D596.
957 doi:10.1093/nar/gks1219

958 Rognes T, Flouri T, Nichols B, Quince C, Mahé F. 2016. VSEARCH: a versatile open
959 source tool for metagenomics. *PeerJ* **4**:e2584. doi:10.7717/peerj.2584

960 Rungue M, Melo V, Martins D, Campos PC, Leles G, Galvão I, Mendes V, Aganetti
961 M, Pedersen Á, Assis NRG. 2021. NLRP6-associated host microbiota
962 composition impacts in the intestinal barrier to systemic dissemination of
963 Brucella abortus. *PLoS Negl Trop Dis* **15**:e0009171.
964 doi:10.1371/journal.pntd.0009171

965 Russell CD, Fairfield CJ, Drake TM, Turtle L, Seaton RA, Wootton Dan G, Sigfrid L,
966 Harrison EM, Docherty AB, de Silva TI, Egan C, Pius R, Hardwick HE, Merson
967 L, Girvan M, Dunning J, Nguyen-Van-Tam JS, Openshaw PJM, Baillie JK,
968 Semple MG, Ho A, Baillie JK, Semple MG, Openshaw PJ, Carson G, Alex B,
969 Bach B, Barclay WS, Bogaert D, Chand M, Cooke GS, Docherty AB, Dunning J,
970 da Silva Filipe A, Fletcher T, Green CA, Harrison EM, Hiscox JA, Ho AY, Horby
971 PW, Ijaz S, Khoo S, Klenerman P, Law A, Lim WS, Mentzer AJ, Merson L,
972 Meynert AM, Noursadeghi M, Moore SC, Palmarini M, Paxton WA, Pollakis G,
973 Price N, Rambaut A, Robertson DL, Russell CD, Sancho-Shimizu V, Scott JT,
974 de Silva T, Sigfrid L, Solomon T, Sriskandan S, Stuart D, Summers C, Tedder
975 RS, Thomson EC, Thompson AR, Thwaites RS, Turtle LC, Gupta RK, Palmieri
976 C, Zambon M, Hardwick H, Donohue C, Lyons R, Griffiths F, Oosthuyzen W,
977 Norman L, Pius R, Drake TM, Fairfield CJ, Knight SR, Mclean KA, Murphy D,
978 Shaw CA, Dalton J, Girvan M, Saviciute E, Roberts S, Harrison J, Marsh L,
979 Connor M, Halpin S, Jackson C, Gamble C, Leeming G, Law A, Wham M,
980 Clohisey S, Hendry R, Scott-Brown J, Greenhalf W, Shaw V, McDonald SE,
981 Keating S, Ahmed KA, Armstrong JA, Ashworth M, Asiimwe IG, Bakshi S,
982 Barlow SL, Booth L, Brennan B, Bullock K, Catterall BW, Clark JJ, Clarke EA,
983 Cole S, Cooper L, Cox H, Davis C, Dincarslan O, Dunn C, Dyer P, Elliott A,
984 Evans A, Finch L, Fisher LW, Foster T, Garcia-Dorival I, Greenhalf W, Gunning
985 P, Hartley C, Jensen RL, Jones CB, Jones TR, Khandaker S, King K, Kiy RT,
986 Koukorava C, Lake A, Lant S, Latawiec D, Lavelle-Langham L, Lefteri D, Lett L,
987 Livoti LA, Mancini M, McDonald S, McEvoy L, McLauchlan J, Metelmann S,
988 Miah NS, Middleton J, Mitchell J, Moore SC, Murphy EG, Penrice-Randal R,
989 Pilgrim J, Prince T, Reynolds W, Ridley PM, Sales D, Shaw VE, Shears RK,
990 Small B, Subramaniam KS, Szemiel A, Taggart A, Tanianis-Hughes J, Thomas
991 Jordan, Trochu E, van Tonder L, Wilcock E, Zhang JE, Flaherty L, Maziere N,
992 Cass E, Doce Carracedo A, Carlucci N, Holmes A, Massey H, Murphy L, Wrobel

993 N, McCafferty S, Morrice K, MacLean A, Adeniji K, Agranoff D, Agwuh K, Ail D,
994 Aldera EL, Alegria A, Angus B, Ashish A, Atkinson D, Bari S, Barlow G, Barnass
995 S, Barrett N, Bassford C, Basude S, Baxter D, Beadsworth M, Bernatoniene J,
996 Berridge J, Best N, Bothma P, Chadwick D, Brittain-Long R, Bulteel N, Burden
997 T, Burtenshaw A, Caruth V, Chadwick D, Chambler D, Chee N, Child J,
998 Chukkambotla S, Clark T, Collini P, Cosgrove C, Cupitt J, Cutino-Moguel M-T,
999 Dark P, Dawson C, Dervisevic S, Donnison P, Douthwaite S, DuRand I,
1000 Dushianthan A, Dyer T, Evans C, Eziefula C, Fegan C, Finn A, Fullerton D,
1001 Garg S, Garg S, Garg A, Gkrania-Klotsas E, Godden J, Goldsmith A, Graham C,
1002 Hardy E, Hartshorn S, Harvey D, Havalda P, Hawcutt DB, Hobrok M, Hodgson
1003 L, Hormis A, Jacobs M, Jain S, Jennings P, Kaliappan A, Kasipandian V, Kegg
1004 S, Kelsey M, Kendall J, Kerrison C, Kerslake I, Koch O, Koduri G, Koshy G,
1005 Laha S, Laird S, Larkin S, Leiner T, Lillie P, Limb J, Linnett V, Little J, Lyttle M,
1006 MacMahon M, MacNaughton E, Mankregod R, Masson H, Matovu E,
1007 McCullough K, McEwen R, Meda M, Mills G, Minton J, Mirfenderesky M,
1008 Mohandas K, Mok Q, Moon J, Moore E, Morgan P, Morris C, Mortimore K,
1009 Moses S, Mpenge M, Mulla R, Murphy M, Nagel M, Nagarajan T, Nelson M,
1010 O'Shea MK, Otahal I, Ostermann M, Pais M, Panchatsharam S,
1011 Papakonstantino D, Paraiso H, Patel B, Pattison N, Pepperell J, Peters M, Phull
1012 M, Pintus S, Singh Pooni J, Post F, Price D, Prout R, Rae N, Reschreiter H,
1013 Reynolds T, Richardson N, Roberts M, Roberts D, Rose A, Rousseau G, Ryan
1014 B, Saluja T, Shah A, Shanmuga P, Sharma A, Shawcross A, Sizer J, Shankar-
1015 Hari M, Smith R, Snelson C, Spittle N, Staines N, Stambach T, Stewart R,
1016 Subudhi P, Szakmany T, Tatham K, Thomas Jo, Thompson C, Thompson R,
1017 Tridente A, Tupper-Carey D, Twagira M, Ustianowski A, Vallotton N, Vincent-
1018 Smith L, Visuvanathan S, Vuylsteke A, Waddy S, Wake R, Walden A, Welters I,
1019 Whitehouse T, Whittaker P, Whittington A, Papineni P, Wijesinghe M, Williams
1020 M, Wilson L, Sarah S, Winchester S, Wiselka M, Wolverson A, Wootton Daniel
1021 G, Workman A, Yates B, Young P. 2021. Co-infections, secondary infections,
1022 and antimicrobial use in patients hospitalised with COVID-19 during the first
1023 pandemic wave from the ISARIC WHO CCP-UK study: a multicentre,
1024 prospective cohort study. *The Lancet Microbe* **2**:e354–e365.
1025 doi:10.1016/S2666-5247(21)00090-2

1026 Saia RS, Giusti H, Luis-Silva F, Pedroso K de JB, Auxiliadora-Martins M, Morejón
1027 KML, Degiovani AM, Cadelca MR, Basile-Filho A. (2021) Clinical investigation of
1028 intestinal fatty acid-binding protein (I-FABP) as a biomarker of SARS-CoV-2
1029 infection. *Int J Infect Dis* **113**:82–86. doi:10.1016/j.ijid.2021.09.051

1030 Sampson TR, Mazmanian SK. 2015. Control of brain development, function, and
1031 behavior by the microbiome. *Cell Host Microbe* **17**:565–76.
1032 doi:10.1016/j.chom.2015.04.011

1033 Santos SS, Miranda VC, Trindade LM, Cardoso VN, Reis DC, Cassali GD, Nicoli JR,
1034 Cara DC, Martins FS. 2021. Bifidobacterium longum subsp. longum 51A
1035 Attenuates Signs of Inflammation in a Murine Model of Food Allergy. *Probiotics*
1036 *Antimicrob Proteins*. doi:10.1007/s12602-021-09846-9

1037 Sencio V, Gallerand A, Gomes Machado M, Deruyter L, Heumel S, Soulard D,
1038 Barthelemy J, Cuinat C, Vieira AT, Barthelemy A, Tavares LP, Guinamard R,
1039 Ivanov S, Grangette C, Teixeira MM, Foligné B, Wolowczuk I, Le Goffic R,
1040 Thomas M, Trottein F. 2021. Influenza Virus Infection Impairs the Gut's Barrier
1041 Properties and Favors Secondary Enteric Bacterial Infection through Reduced
1042 Production of Short-Chain Fatty Acids. *Infect Immun* **89**:e0073420.
1043 doi:10.1128/IAI.00734-20

1044 Song SJ, Lauber C, Costello EK, Lozupone CA, Humphrey G, Berg-Lyons D,
1045 Caporaso JG, Knights D, Clemente JC, Nakielny S, Gordon JI, Fierer N, Knight
1046 R. 2013. Cohabiting family members share microbiota with one another and with
1047 their dogs. *Elife* **2**. doi:10.7554/eLife.00458

1048 Souza DG, Vieira AT, Soares AC, Pinho V, Nicoli JR, Vieira LQ, Teixeira MM. 2004.
1049 The essential role of the intestinal microbiota in facilitating acute inflammatory
1050 responses. *J Immunol* **173**:4137–4146.

1051 Subramanian A, Nirantharakumar K, Hughes S, Myles P, Williams T, Gokhale KM,
1052 Taverner T, Chandan JS, Brown K, Simms-Williams N. 2022. Symptoms and
1053 risk factors for long COVID in non-hospitalized adults. *Nat Med* **28**:1706–1714.
1054 doi: 10.1038/s41591-022-01909-w

1055 Taquet M, Geddes JR, Husain M, Luciano S, Harrison PJ. 2021. 6-month
1056 neurological and psychiatric outcomes in 236 379 survivors of COVID-19: a
1057 retrospective cohort study using electronic health records. *The lancet Psychiatry*
1058 **8**:416–427. doi:10.1016/S2215-0366(21)00084-5

1059 Van Laethem J, Wuyts S, Van Laere S, Koulalis J, Colman M, Moretti M, Seyler L,
1060 De Waele E, Pierard D, Lacor P, Allard S. 2022. Antibiotic prescriptions in the
1061 context of suspected bacterial respiratory tract superinfections in the COVID-19
1062 era: a retrospective quantitative analysis of antibiotic consumption and
1063 identification of antibiotic prescription drivers. *Intern Emerg Med* **17**:141–151.
1064 doi:10.1007/s11739-021-02790-0

1065 Vieira A.T., Galvão I, Amaral FA, Teixeira MM, Nicoli JR, Martins FS. 2015. Oral
1066 treatment with Bifidobacterium longum 5 1A reduced inflammation in a murine
1067 experimental model of gout. *Benef Microbes* **6**:799–806.
1068 doi:10.3920/BM2015.0015

1069 Vieira Angélica T, Macia L, Galvão I, Martins FS, Canesso MCC, Amaral FA, Garcia
1070 CC, Maslowski KM, De Leon E, Shim D, Nicoli JR, Harper JL, Teixeira MM,
1071 Mackay CR. 2015. A Role for Gut Microbiota and the Metabolite-Sensing
1072 Receptor GPR43 in a Murine Model of Gout. *Arthritis Rheumatol (Hoboken, NJ)*
1073 **67**:1646–1656. doi:10.1002/art.39107

1074 Vieira AT, Rocha VM, Tavares L, Garcia CC, Teixeira MM, Oliveira SC, Cassali GD,
1075 Gamba C, Martins FS, Nicoli JR. 2016a. Control of Klebsiella pneumoniae
1076 pulmonary infection and immunomodulation by oral treatment with the
1077 commensal probiotic Bifidobacterium longum 51A. *Microbes Infect* **18**:180–189.
1078 doi:10.1016/j.micinf.2015.10.008

1079 Vieira AT, Rocha VM, Tavares L, Garcia CC, Teixeira MM, Oliveira SC, Cassali GD,
1080 Gamba C, Martins FS, Nicoli JR. 2016b. Control of Klebsiella pneumoniae
1081 pulmonary infection and immunomodulation by oral treatment with the
1082 commensal probiotic Bifidobacterium longum 51A. *Microbes Infect* **18**:180–189.
1083 doi:10.1016/j.micinf.2015.10.008

1084 WHO. 2023. COVID-19 weekly epidemiological update, edition 134, 16 March 2023.

1085 Wu T, Xu F, Su C, Li H, Lv N, Liu Y, Gao Y, Lan Y, Li J. 2020. Alterations in the gut
1086 microbiome and cecal metabolome during Klebsiella pneumoniae-induced
1087 pneumosepsis. *Front Immunol* **11**:1331. doi: 10.3389/fimmu.2020.01331

1088 Wu Y, Cheng X, Jiang G, Tang H, Ming S, Tang L, Lu J, Guo C, Shan H, Huang X.
1089 2021a. Altered oral and gut microbiota and its association with SARS-CoV-2
1090 viral load in COVID-19 patients during hospitalization. *npj Biofilms Microbiomes*
1091 **7**:61. doi:10.1038/s41522-021-00232-5

1092 Wu Y, Cheng X, Jiang G, Tang H, Ming S, Tang L, Lu J, Guo C, Shan H, Huang X.
1093 2021b. Altered oral and gut microbiota and its association with SARS-CoV-2
1094 viral load in COVID-19 patients during hospitalization. *npj Biofilms Microbiomes*
1095 **7**:90. doi:10.1038/s41522-021-00262-z

1096 Xu E, Xie Y, Al-Aly Z. 2023. Long-term gastrointestinal outcomes of COVID-19. *Nat*
1097 *Commun* **14**:983. doi:10.1038/s41467-023-36223-7

1098 Yang I, Arthur RA, Zhao L, Clark J, Hu Y, Corwin EJ, Lah J. 2021. The oral
1099 microbiome and inflammation in mild cognitive impairment. *Exp Gerontol*
1100 **147**:111273. doi:10.1016/j.exger.2021.111273

1101 Yeoh YK, Zuo T, Lui GC-Y, Zhang F, Liu Q, Li AY, Chung AC, Cheung CP, Tso EY,
1102 Fung KS, Chan V, Ling L, Joynt G, Hui DS-C, Chow KM, Ng SSS, Li TC-M, Ng
1103 RW, Yip TC, Wong GL-H, Chan FK, Wong CK, Chan PK, Ng SC. 2021. Gut
1104 microbiota composition reflects disease severity and dysfunctional immune
1105 responses in patients with COVID-19. *Gut* **70**:698–706. doi:10.1136/gutjnl-2020-
1106 323020

1107 Yuan L, Hensley C, Mahsoub HM, Ramesh AK, Zhou P. 2020. Microbiota in viral
1108 infection and disease in humans and farm animals. pp. 15–60.
1109 doi:10.1016/bs.pmbts.2020.04.005

1110 Zhang F, Wan Y, Zuo T, Yeoh YK, Liu Q, Zhang L, Zhan H, Lu W, Xu W, Lui GCY, Li
1111 AYL, Cheung CP, Wong CK, Chan PKS, Chan FKL, Ng SC. 2022. Prolonged
1112 Impairment of Short-Chain Fatty Acid and L-Isoleucine Biosynthesis in Gut
1113 Microbiome in Patients With COVID-19. *Gastroenterology* **162**:548-561.e4.

doi:10.1053/j.gastro.2021.10.013

Zheng D, Liwinski T, Elinav E. 2020. Interaction between microbiota and immunity in health and disease. *Cell Res* **30**:492–506. doi:10.1038/s41422-020-0332-7

Zollner A, Koch R, Jukic A, Pfister A, Meyer M, Rössler A, Kimpel J, Adolph TE, Tilg H. 2022. Post-acute COVID-19 is characterized by gut viral antigen persistence in inflammatory bowel diseases. *Gastroenterology*. doi:10.1053/j.gastro.2022.04.037

Zuo T, Liu Q, Zhang F, Lui GCY, Tso EYK, Yeoh YK, Chen Z, Boon SS, Chan FKL, Chan PKS, Ng SC. 2021. Depicting SARS-CoV-2 faecal viral activity in association with gut microbiota composition in patients with COVID-19. *Gut* **70**:276–284. doi:10.1136/gutjnl-2020-322294

Figure legends

Figure 1. Clinical characteristics and food habits were associated with gut microbiota composition and an antimicrobial resistance profile in *Enterobacteriaceae* species of post-COVID and control human subjects. (**A**) Experimental design: collection of feeding habits, clinic survey, and fecal microbiota composition analysis of 59 control and 72 post-COVID subjects (N=131). (**B**) Co-morbidities in control and post-COVID groups. (**C**) Feeding composition (N=131). (**D**) Antibiotic-treated control and post-COVID subjects (N=131). (**E**) SARS-CoV-2 quantification by RT-qPCR in the feces of control and post-COVID subjects, a.u.: arbitrary units (N=131). (**F**) 16S rRNA sequencing of gut microbiota from control and post-COVID subjects at the family level (N=44). Principal Component Analysis based on weighted Unifrac distances (p = 0.900), a β-diversity index (N=44). α-diversity analysis based on Shannon, Simpson, and Chao1 indexes (N=44)**.** (**G**) *Enterobacteriaceae* quantification in fecal samples of the subjects (N=131). (**H**) Frequency of *Enterobacteriaceae* strains present in the fecal samples of human subjects as multidrug-resistant, resistant, or non-resistance (N=131). Statistical analysis: Fisher's exact test was used in D, Wilcoxon and PerMANOVA pairwise tests were used in F, Unpaired Student's *t*-test was used in G, and Chi-square test was used in H. Data are shown as mean and standard deviation (SD).

Figure 1 – Figure supplement 1. Workflow and flowchart for the collection and analysis of post-COVID and control human samples, and analysis of resistant *Enterobacteriaceae* species in human fecal samples. (**A**) Analysis of feeding habits sociodemographic, antibiotics use (at least 4 months before the application of sample collection), and clinical parameters of 59 control and 72 post-COVID subjects. Fresh feces were collected and subjected to SARS-CoV-2 quantification by RT-qPCR, 16S rRNA sequencing, SCFA's measurements, cultivating fecal microbiota, and antimicrobial susceptibility tests. (**B**) Flowchart of the human samples. (**C**) Descriptive analysis of percentage of resistant *Enterobacteriaceae* species (N=131).

Figure 2. Control and post-COVID fecal microbiota transplant and effects on the gut of post-COVID mice. (**A**) Experimental design: control (N=8) and post-COVID (N=14) mice received fresh feces from donors, and then analyzes of the gut microbiota and

colon histology were performed 12 days after FMT. (**B**) 16S rRNA sequencing and comparison of the gut microbiota composition between human donor and mouse that received FMT. Principal Component Analysis based on weighted Unifrac distances, a β-diversity index. α-diversity analysis based on Shannon, Simpson, and Chao1 indexes (Donors N=19; Mice N=19). (**C**) 16S rRNA sequencing of gut microbiota of control and post-COVID mice after FMT. β-diversity and α-diversity (N=19). (**D**) Differential bacterial abundance in feces of control and post-COVID mice, *Lachonospiraceae* (p = 0.0300) (N=19). (**E**) Histological alterations in the large intestine in mice that received FMT. Black arrows indicate increases in Colonic Lymphoid Patches (N=8). Red arrows Graphs showing the Colonic Lymphoid Patches Perimeter and the ratio between Goblet cells and Epithelial cells in the colon. Statistical analysis: Wilcoxon test was used in B and C, PerMANOVA pairwise test was used in B and C, unpaired Student's-*t* test was used in D, and Wald test was used in E. Data are shown as mean and standard deviation (SD). All results are representative of three independent experiments.

Figure 2 – Figure supplement 1. Altered in the intestinal homeostasis of post-COVID subjects compared to controls from the same household. (**A**) The FMT workflow of control and post-COVID donors performed individually for germ-free mice. (**B**) Quantification of serum endotoxin (LPS) levels (N=14). (**C**) Serum I-FABP levels (N=24). Fecal (**D**) acetate, (**E**) propionate, and (**F**) butyrate levels in cohousing post-COVID and controls subjects (N= 24). Statistical analysis: paired Student's-*t* test was used in A-E. Data are shown as mean and standard deviation (SD).

Figure 3. Post-COVID gut microbiota induce lung alterations in HM mice. (**A**) Experimental design: germ-free mice received fresh feces from control (N=8) or post-COVID (N=14) donors and lung tissue and bronchoalveolar lavage were assessed 12 days after FMT. (**B**) H&E staining: the histopathological lung alterations induced by FMT to HM GF mice. Graph showing the histopathological score of airways, vascular and parenchymal inflammation in control and post-COVID mice lungs. Arrowheads indicate lung airways. Asterisks indicate inflammatory infiltrates. Scale bar: 50μm. 20X objective (N=22). α-SMA immune-staining: lung samples from HM GF mice and graph showing the morphometrical analysis of muscular layer changes. Ten images of the muscular layer of each animal were acquired with a 40X objective.

Arrowheads indicate the immunostained area (N=10). (**C**) Total number of cells in bronchoalveolar lavage (N=19). (**D**) Cultivable *Enterobacteriaceae* load in bronchoalveolar lavage (N=19). (**E**) RT-qPCR for SARS-CoV-2 in the lungs of control and post-COVID mice (N=22). Statistical analysis: unpaired Student's *t*-test was used in B, C and D. Data are shown as mean and standard deviation (SD). All results are representative of three independent experiments.

Figure 4. FMT from Post-COVID patients impacts the gut-lung axis and increases susceptibility to *K. pneumoniae* B31 lung infection. (**A**) Experimental design: germ-free mice received fresh feces from control or post-COVID donors and were infected with *K. pneumoniae* B31 (*K. pneumoniae:* control N=13, post-COVID N=15) or received saline (vehicle), and lung tissue, bronchoalveolar lavage and serum SCFAs levels were assessed. (**B**) Histological alterations in the lung of post-COVID mice infected by *K. pneumoniae* B31 and graph showing the histopathological score of the airway, vascular and parenchymal inflammation in control and post-COVID mice lungs (N=28). Asterisks indicate inflammatory infiltrates. Hash marks areas of emphysema. Scale bar: 50µm. 20X and 40X objective. (**C**) Total number of inflammatory cells in bronchoalveolar lavage (BAL) (N=28). (**D**) Total numbers of *Enterobacteriaceae* in BAL (N=28). (**E**) Serum acetate levels ($mmol.L^{-1}$) in vehicle and *K. pneumonia* infected HM mice (N=33). Statistical analysis: unpaired Student's *t*-test was used in B and C, Mann-Whitney test was used in D and Two-way ANOVA with Tukey's tests was used in E. Data are shown as mean and standard deviation (SD). All results are representative of three independent experiments.

Figure 5. FMT from Post-COVID patients induces cognitive alterations in HM mice. (**A**) Experimental design: germ-free mice received fresh feces from control (N=14) or post-COVID (N=15) donors, and underwent cognition (object location and recognition) tests nine days later. Following behavioral analysis, their hippocampus was subjected to mRNA expression. (**B**) Percentage of exploration time for the new object (N) or the one remaining unmoved (O) in the location test relative to a total exploration time (N=29) 9 days after FMT. Quantification of the expression, by RT-qPCR, of (**C**) TNF (N=13), (**D**) BDNF (N=13), and (**E**) PSD95 (N=13) in the hippocampus 12 days after FMT. Statistical analysis: One sample *t* test against the hypothetical value of 50% and unpaired Student's *t* test was used in B. Data are

shown as mean and standard deviation (SD). All results are representative of two independent experiments.

Figure 6. The mouse model of MHV-3 infection showed memory impairment in object recognition and location tests, and treatment with *B. longum* 5^{1A} reversed the cognitive alterations. (**A**) Experimental design: C57BL/6 non-infected and MHV-3 infected and treated with probiotic *B. longum* 5^{1A} (Vehicle: non-infected N=4; MHV-3 infected N=7; *B. longum* 5^{1A}: non-infected N=4; MHV-3 infected N=5), and subjected to behavioral (object location and recognition) tests 4 days later. (**B**) Percentage of exploration time for the new object (N) or the one remaining unmoved (O) in the location test relative to a total exploration time (N= 20). Statistical analysis: One sample *t* test against the hypothetical value of 50%. Data are shown as mean and standard deviation (SD).

1234 **Tables**

Table 1: Clinical and demographic characteristics of all human subjects in the study.

Parameters	Non-COVID-19	Assymptomatic	Symptomatic
Gender, n (%)	n = 59 (45.0%)	n = 8 (6.1%)	n = 64 (48.8%)
Male	19 (32.2%)	2 (25.0%)	24 (37.5%)
Female	40 (67.8%)	6 (75.0%)	40 (62.5%)
Age Group, n (%)			
<18 years	3 (5.1%)	-	2 (3.1%)
18-39 years	43 (72.9%)	3 (37.5%)	45 (70.3%)
40-49 years	5 (8.5%)	2 (25.0%)	11 (17.2%)
50-59 years	7 (11.9%)	3 (37.5%)	5 (7.8%)
> 60 years	1 (1.7%)	-	1 (1.7%)
Body Mass Index, n (%)			
Underweight	2 (3.4%)	1 (12.5%)	4 (6.2%)
Normal weight	29 (49.15%)	3 (37.5%)	31 (48.4%)
Overweight	19 (32.2%)	3 (37.5%)	20 (31.2%)
Obesity class I	4 (6.8%)	-	8 (12.5%)
Obesity class II	3 (5.1%)	-	1 (1.6%)
Symptoms during COVID-19, n (%)			
Headache	-	-	47 (73.4%)
Fadigue	-	-	45 (70.3%)
Cough	-	-	40 (62.5%)
Anosmia	-	-	39 (60.9%)
Coryza or stuffy nose	-	-	37 (57.8%)
Myalgia	-	-	37 (57.8%)
Dysgeusia	-	-	36 (56.2%)
Fever ≥ 37,8ºC	-	-	29 (45.3%)
Chills	-	-	21 (32.8%)
Sore throat	-	-	20 (31.2%)
Dyspnea	-	-	12 (18.7%)
Conjunctivitis	-	-	3 (4.7%)
Gastrointestinal symptoms, n (%)			
Diarrhea	-	-	22 (34.4%)
Appetite loss	-	-	19 (29.7%)
Nausea	-	-	11 (17.2%)
Abdominal pain	-	-	7 (10.9%)
Vomiting	-	-	3 (4.7%)

1235

Table 2: Food characteristics used for the feeding score.

Group	Food group	Characteristics
A	**Ultraprocced food**	Chocolate, ice cream, pudding, mousse, cereal bar
		Sausage, salami, bologna, sausage, hamburger, turkey meat, chorizo
		Mayonnaise, margarine, whipped cream
		Ready sauces, frozen and ready-to-heat products
		Breads, cakes and cookies
		Pizza, French Fries, Chips, Instant Noodles
B	**Fiber source foods**	Fruits (Papaya, pear, grape, mango, guava, tangerine, pineapple, plum, watermelon, avocado, jabuticaba, acerola)
		Vegetables (Pumpkin, carrot, okra, chayote, cucumber, pepper, eggplant, pumpkin, cabbage, cauliflower, broccoli, radish, green beans, potato, Lettuce, cabbage, chicory, taioba, mustard, spinach, watercress, chard)
C	**Functional foods**	Beans, soy
		Oatmeal, honey, roll, curd
		Banana, apple, orange, lemon
		Tomatoes, beets, sweet potatoes, yacon potatoes, sauerkraut
		Soluble fiber (Garlic, Onion, Garlic)
		Probiotics (Yakult, Activia, Actimel, Kefir, Chamyto, Simfort)

1236

Table 3: Primer sequences for RT-qPCR

Gene Name	Forward primer (5'-3')	Reverse primer (5'-3')
IL-1β	TTGACGGACCCCAAAAGAT	GAAGCTGGATGCTCTCATCTG
IL6	GATGGATGCTACCAAACTGGA	CCAGGTAGCTATGGTACTCCAGAA
TNF¹	TGCTGGGAAGCCTAAAAGG	CGAATTTTGAGAAGATGATCCTG
TNF²	GCTGAGCTCAAACCCTGGTA	CGGACTCCGCAAAGTCTAAG
IFNβ	GCCCTGTAGGTGAGGTTGATCT	AGCTCCAAGAAAGGACGAACAT
PSD-95–Dgl4	TCTGTGCGAGAGGTAGCAGA	AAGCACTCCGTGAACTCCTG
BDNF	ATGAAAGAAGTAAACGTCCAC	CCAGCAGAAAGAGTAGAGGAG
RpL32	GCTGCCATCTGTTTTACGG	TGACTGGTGCCTGATGAACT
MHV-3	CAGATCCTTGATGATGGCGTAGT	AGAGTGTCCTATCCCGACTTTCTC

Note:¹Primer used for RT-PCR in lung and gut samples; ² Primer used for RT-PCR in brain samples; IL, interleukin; TNF, Tumor necrosis factor; IFN, interferon; PSD-95–Dgl4, Post-synaptic density protein; BDNF, Brain-derived neurotrophic factor; RpL, Ribosomal protein; MHV-3, Murine Hepatitis Virus-3 nucleocapsid protein (N) gene.

1237

Figure1

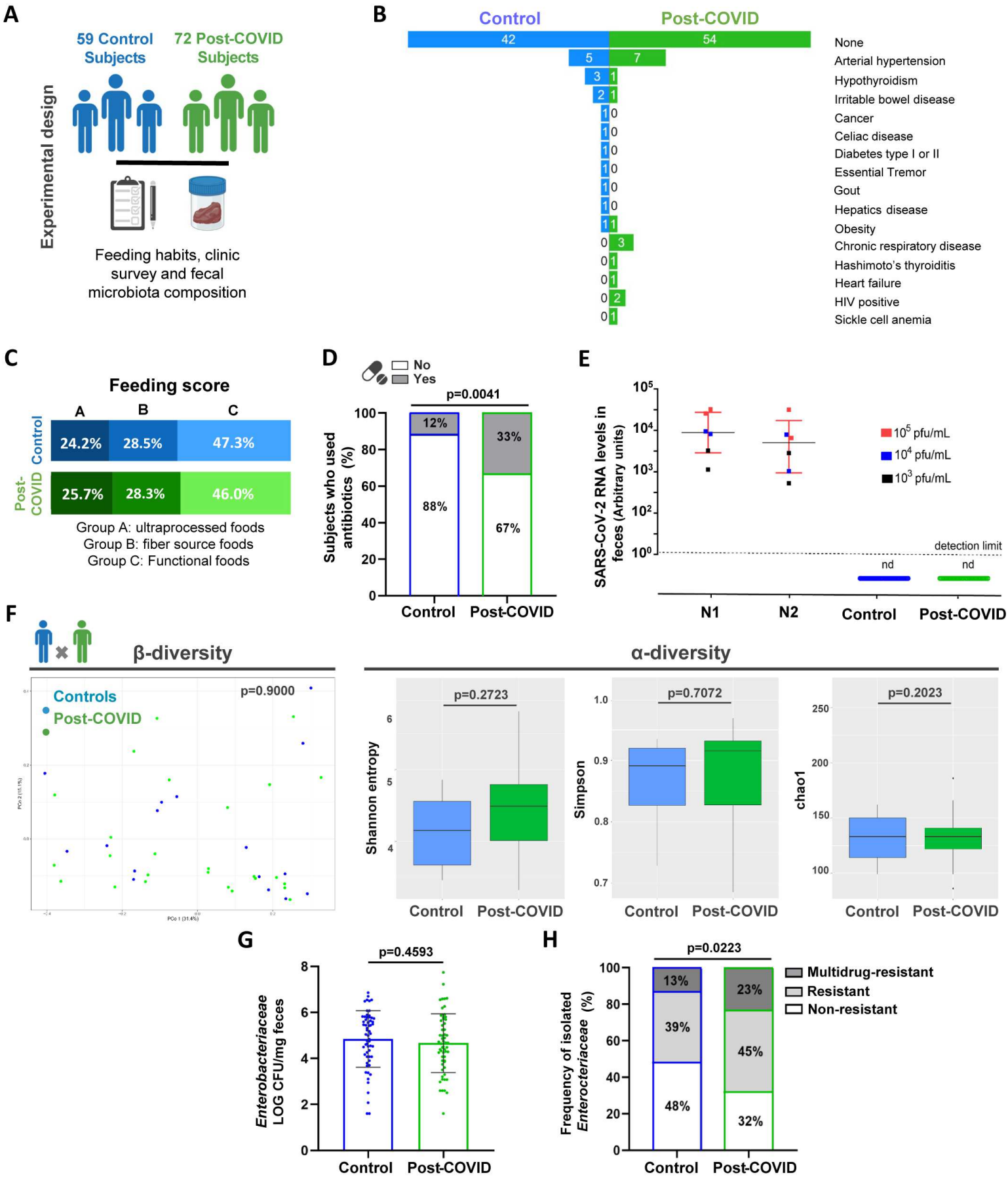
A
59 Control Subjects
72 Post-COVID Subjects
Experimental design
Feeding habits, clinic survey and fecal microbiota composition
B
Control
Post-COVID
None
Arterial hypertension
Hypothyroidism
Irritable bowel disease
Cancer
Celiac disease
Diabetes type I or II
Essential Tremor
Gout
Hepatics disease
Obesity
Chronic respiratory disease
Hashimoto's thyroiditis
Heart failure
HIV positive
Sickle cell anemia
C
Feeding score
A
B
C
Control
Post-COVID
24.2%
28.5%
47.3%
25.7%
28.3%
46.0%
Group A: ultraprocessed foods
Group B: fiber source foods
Group C: Functional foods
D
No
Yes
p=0.0041
Subjects who used antibiotics (%)
12%
33%
88%
67%
Control
Post-COVID
E
SARS-CoV-2 RNA levels in feces (Arbitrary units)
10^5 pfu/mL
10^4 pfu/mL
10^3 pfu/mL
detection limit
nd
nd
N1
N2
Control
Post-COVID
F
β-diversity
Controls
Post-COVID
p=0.9000
α-diversity
p=0.2723
Shannon entropy
p=0.7072
Simpson
p=0.2023
chao1
Control
Post-COVID
G
p=0.4593
Enterobacteriaceae LOG CFU/mg feces
Control
Post-COVID
H
p=0.0223
Frequency of isolated Enterocteriaceae (%)
Multidrug-resistant
Resistant
Non-resistant
13%
39%
48%
23%
45%
32%
Control
Post-COVID

Figure 1 - figure supplement 1

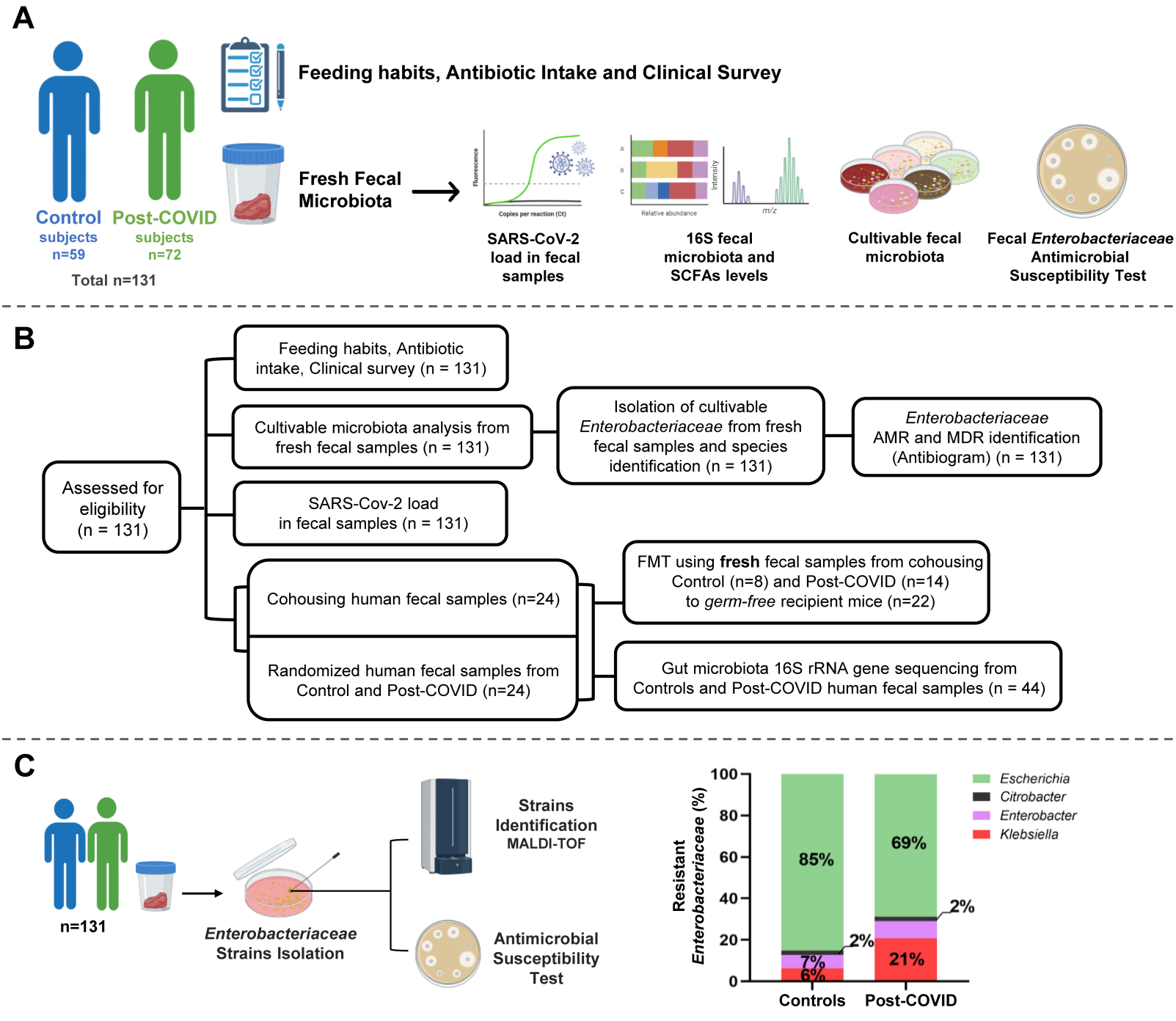

Figure 2.

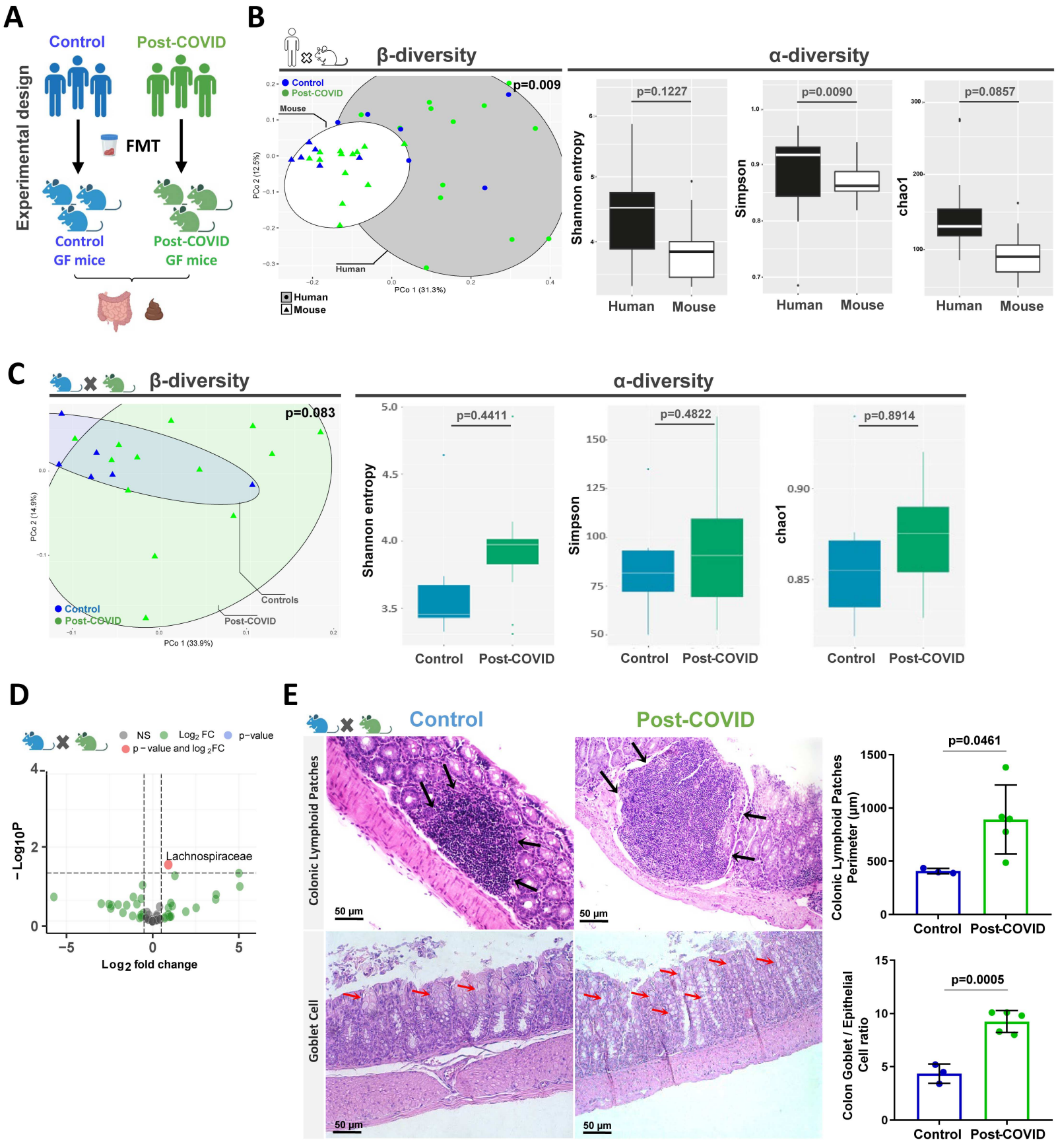
A
Control
Post-COVID
Experimental design
FMT
Control GF mice
Post-COVID GF mice
B
β-diversity
α-diversity
p=0.009
Control
Post-COVID
Mouse
Human
PCo 1 (31.3%)
PCo 2 (12.5%)
p=0.1227
p=0.0090
p=0.0857
Shannon entropy
Simpson
chao1
Human
Mouse
C
β-diversity
α-diversity
p=0.083
PCo 1 (33.9%)
PCo 2 (14.9%)
Controls
Post-COVID
p=0.4411
p=0.4822
p=0.8914
Shannon entropy
Simpson
chao1
Control
Post-COVID
D
NS
Log2 FC
p−value
p − value and log 2FC
−Log10P
Lachnospiraceae
Log2 fold change
E
Control
Post-COVID
Colonic Lymphoid Patches
Goblet Cell
50 μm
p=0.0461
Colonic Lymphoid Patches Perimeter (μm)
p=0.0005
Colon Goblet / Epithelial Cell ratio

Figure 2 - figure supplement 2

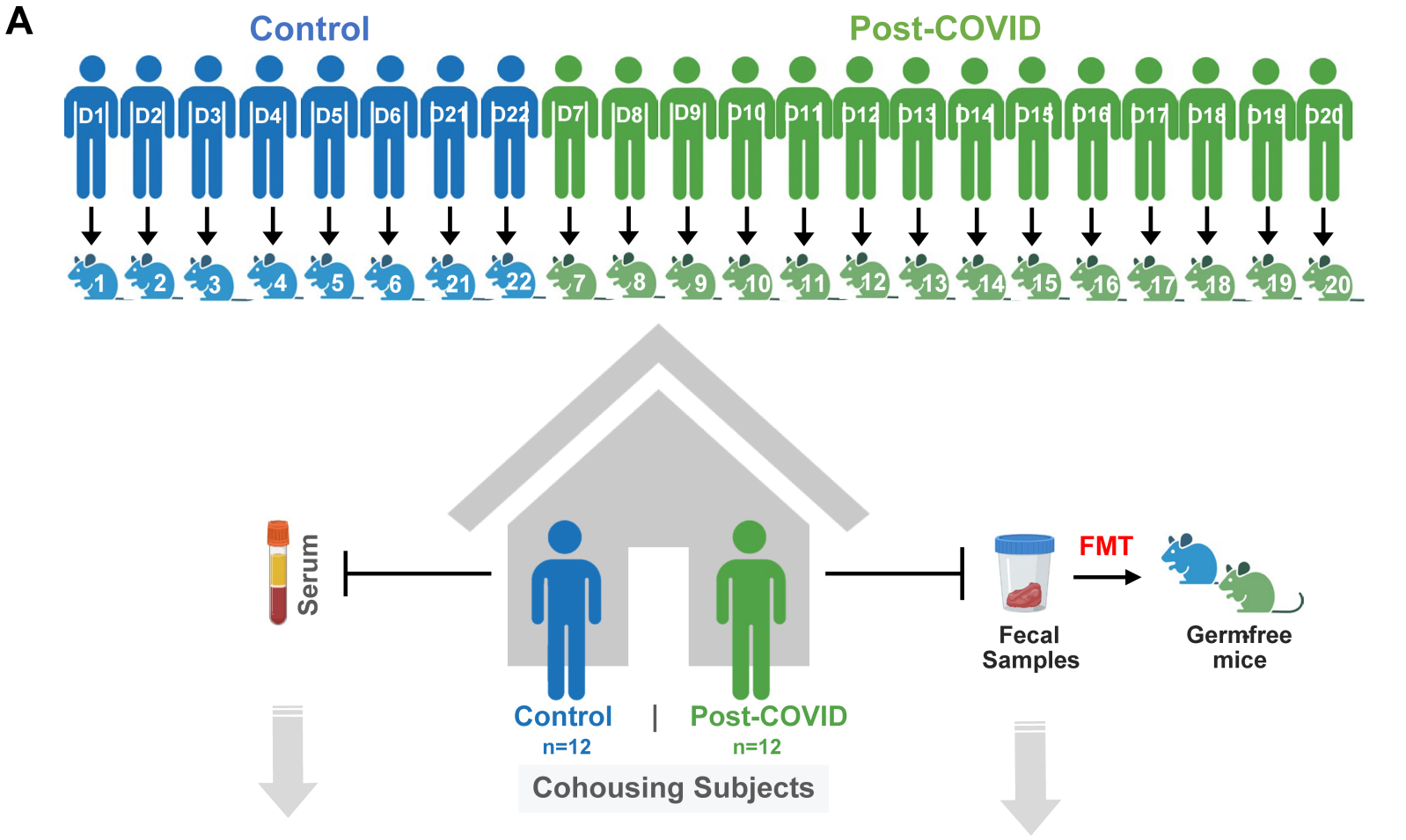

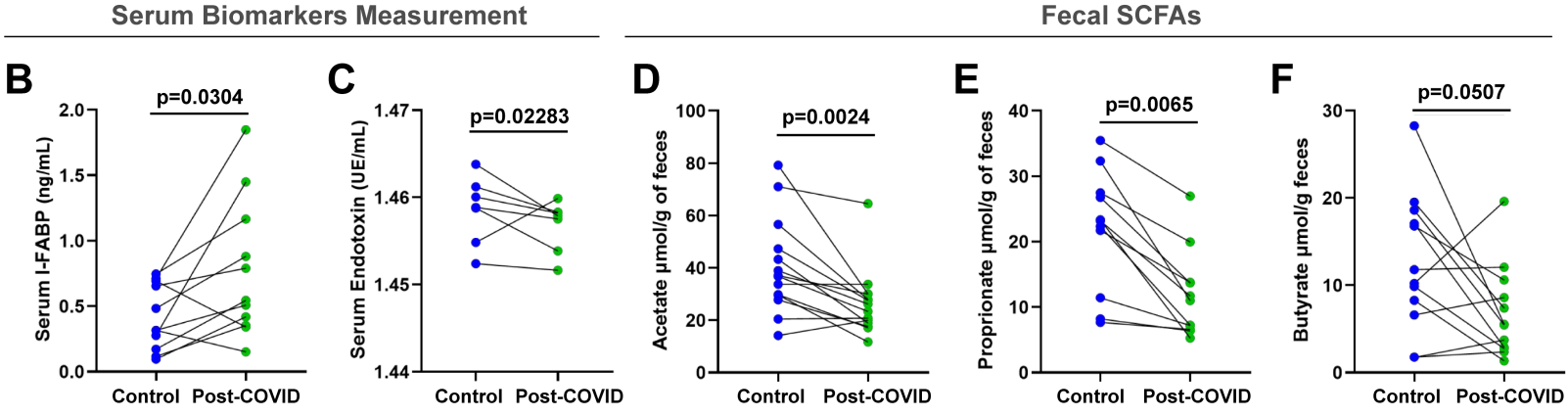

Figure 3.

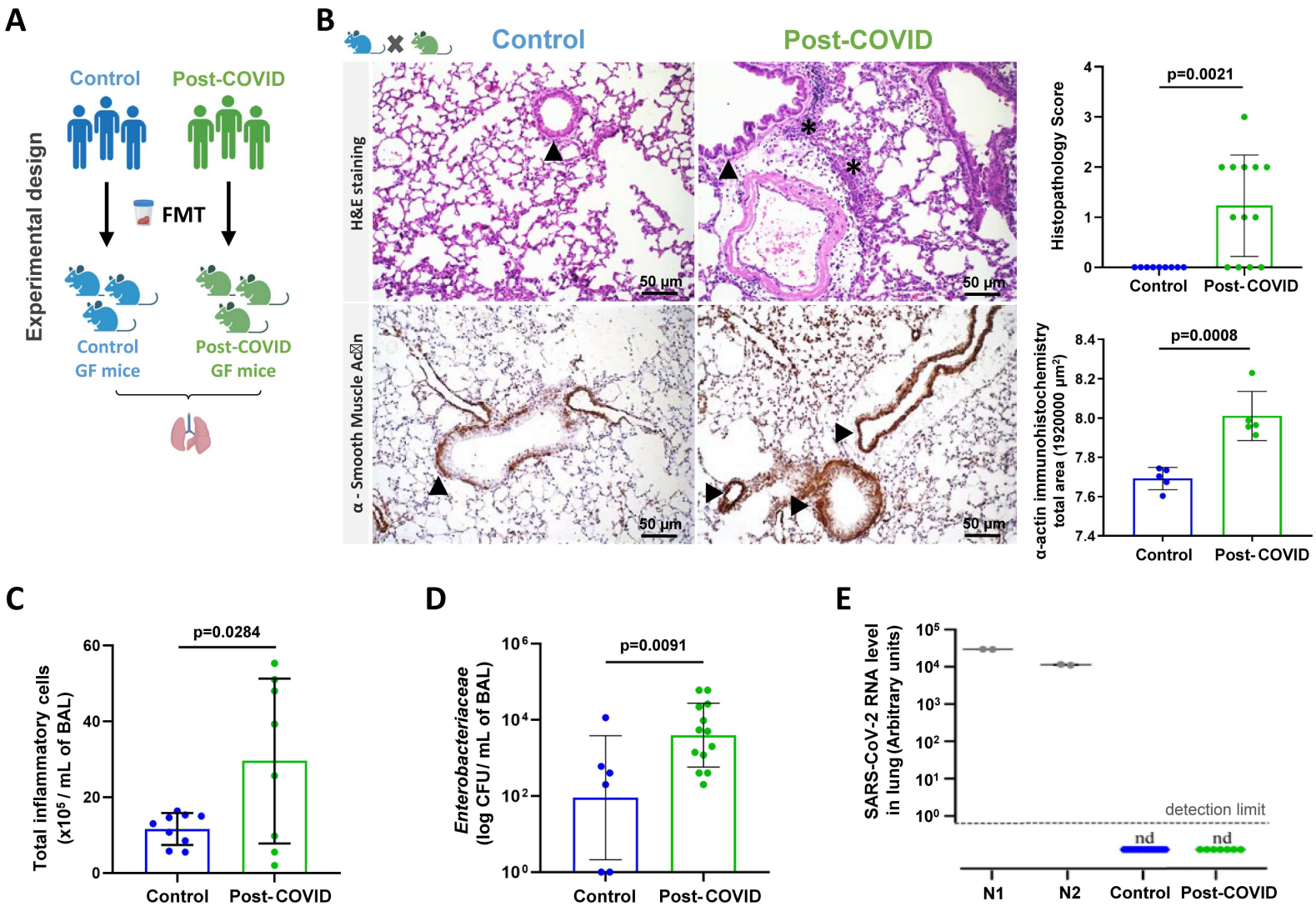
A
Experimental design
Control
Post-COVID
FMT
Control GF mice
Post-COVID GF mice
B
Control
Post-COVID
H&E staining
α - Smooth Muscle Actin
50 µm
Histopathology Score
p=0.0021
Control
Post-COVID
α-actin immunohistochemistry total area (1920000 µm²)
p=0.0008
C
Total inflammatory cells (x10⁵ / mL of BAL)
p=0.0284
D
Enterobacteriaceae (log CFU/ mL of BAL)
p=0.0091
E
SARS-CoV-2 RNA level in lung (Arbitrary units)
detection limit
nd
N1
N2

Figure 4.

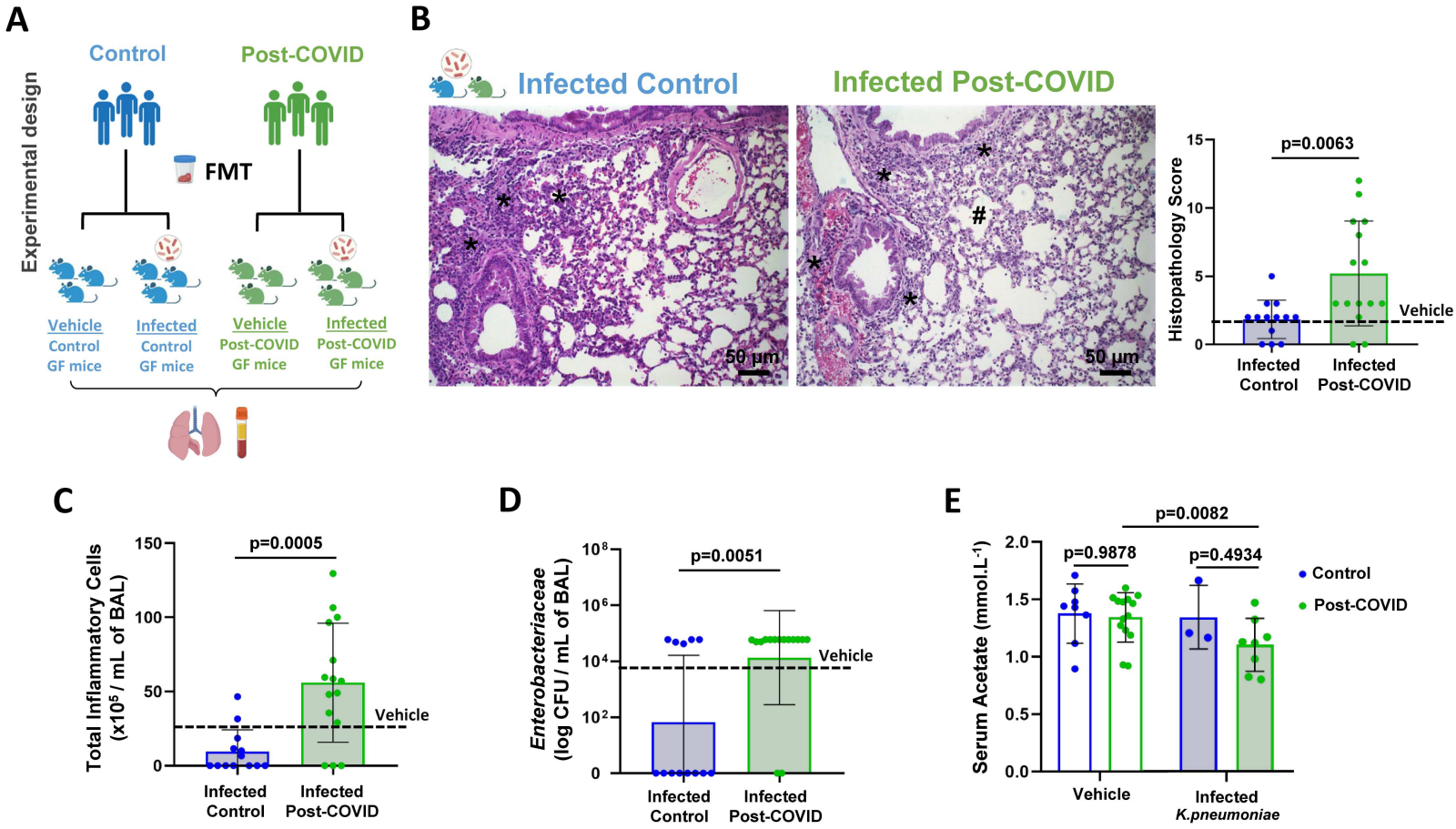
A
Experimental design
Control
Post-COVID
FMT
Vehicle Control GF mice
Infected Control GF mice
Vehicle Post-COVID GF mice
Infected Post-COVID GF mice
B
Infected Control
Infected Post-COVID
50 µm
50 µm
Histopathology Score
p=0.0063
Vehicle
Infected Control
Infected Post-COVID
C
Total Inflammatory Cells (x10⁵ / mL of BAL)
p=0.0005
Vehicle
Infected Control
Infected Post-COVID
D
Enterobacteriaceae (log CFU / mL of BAL)
p=0.0051
Vehicle
Infected Control
Infected Post-COVID
E
Serum Acetate (mmol.L⁻¹)
p=0.0082
p=0.9878
p=0.4934
Control
Post-COVID
Vehicle
Infected K.pneumoniae

Figure 5.

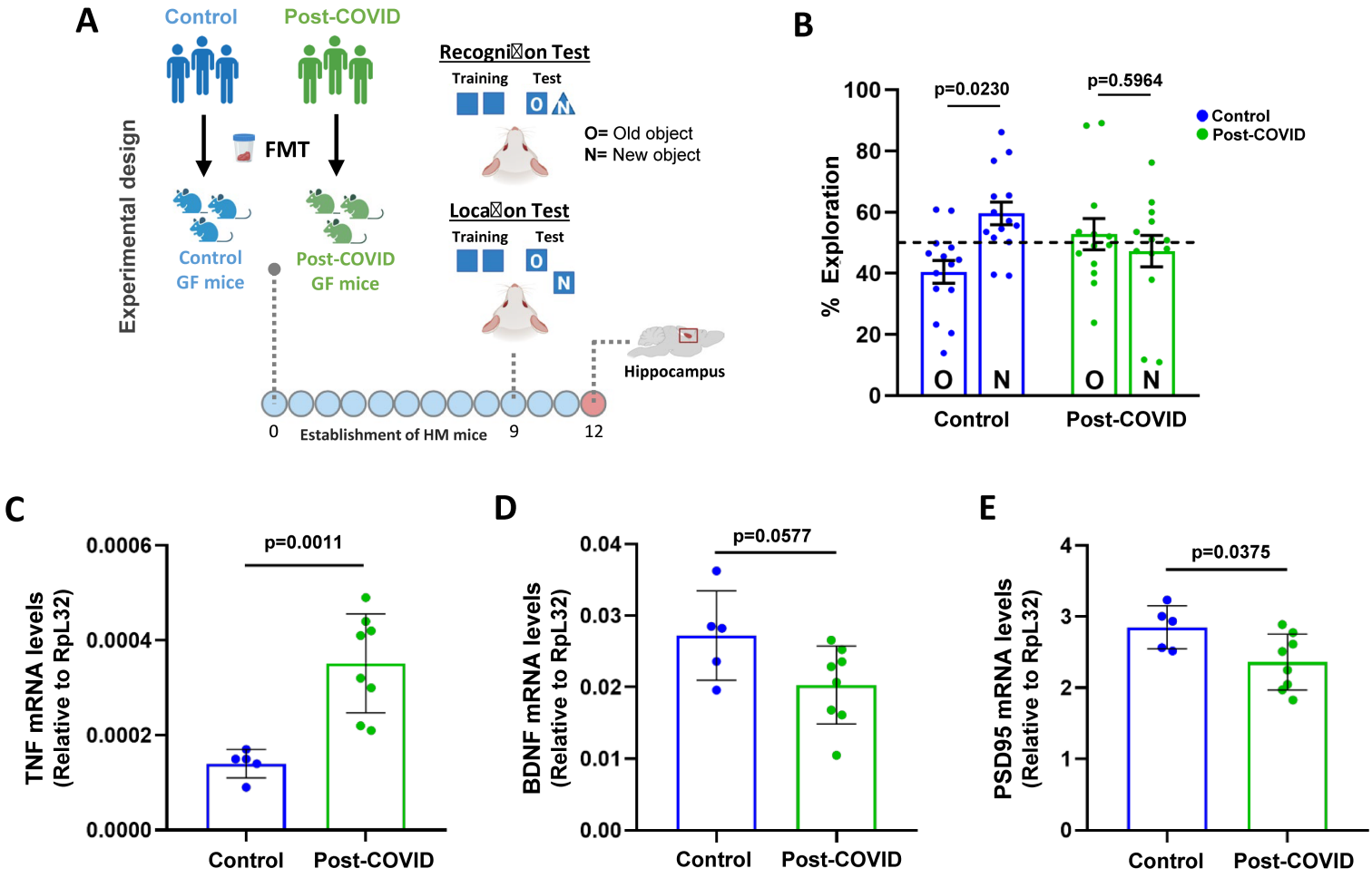
A
Control
Post-COVID
Experimental design
FMT
Control GF mice
Post-COVID GF mice
Recogni⊠on Test
Training
Test
O= Old object
N= New object
Loca⊠on Test
Hippocampus
0
Establishment of HM mice
9
12
B
% Exploration
p=0.0230
p=0.5964
Control
Post-COVID
O
N
C
TNF mRNA levels (Relative to RpL32)
p=0.0011
D
BDNF mRNA levels (Relative to RpL32)
p=0.0577
E
PSD95 mRNA levels (Relative to RpL32)
p=0.0375

Figure 6.

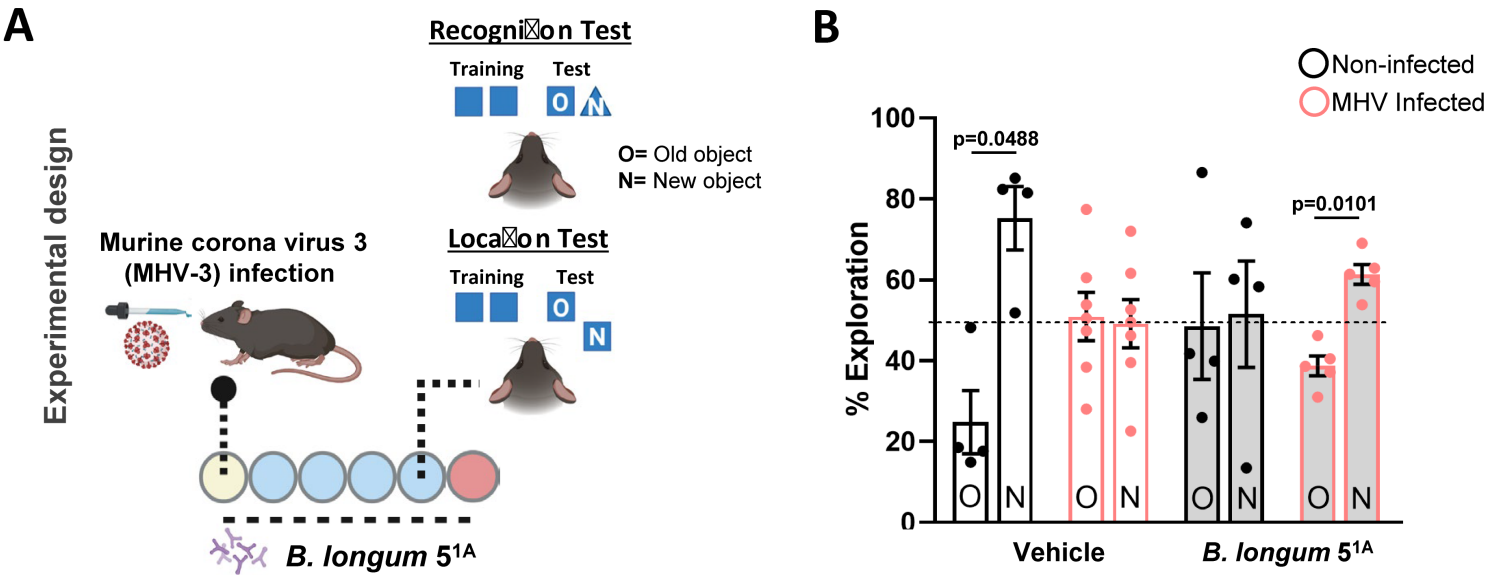
A
Experimental design
Murine corona virus 3
(MHV-3) infection
B. longum 5^1A
Recogni⊠on Test
Training
Test
O
N
O= Old object
N= New object
Loca⊠on Test
Training
Test
O
N
B
Non-infected
MHV Infected
% Exploration
100
80
60
40
20
0
p=0.0488
p=0.0101
O
N
O
N
O
N
O
N
Vehicle
B. longum 5^1A

Supplementary Files

This is a list of supplementary files associated with this preprint. Click to download.

- Figure1figuresupplement1.tif
- Figure1figuresupplement1.tif